SEISMIC DESIGN GUIDE FOR MASONRY BUILDINGS

APPENDICES

Donald Anderson ***Svetlana Brzev***

Canadian Concrete Masonry Producers Association

Canadian Concrete Masonry Producers Association
Region 6 of the National Concrete Masonry Association
CCMPA
Building Strength

April 2009

DISCLAIMER

While the authors have tried to be as accurate as possible, they cannot be held responsible for the designs of others that might be based on the material presented in this document. The material included in this document is intended for the use of design professionals who are competent to evaluate the significance and limitations of its contents and recommendations and able to accept responsibility for its application. The authors, and the Canadian Concrete Masonry Producers Association, disclaim any and all responsibility for the applications of the stated principles and for the accuracy of any of the material included in the document.

AUTHORS

Don Anderson, Ph.D., P.Eng.
Department of Civil Engineering,
University of British Columbia
Vancouver, BC

Svetlana Brzev, Ph.D., P.Eng.
Department of Civil Engineering
British Columbia Institute of Technology
Burnaby, BC

TECHNICAL EDITORS

Gary Sturgeon, P.Eng., Director of Technical Services, CCMPA
Bill McEwen, P.Eng., LEED AP, Executive Director, Masonry Institute of BC
Dr. Mark Hagel, EIT, Technical Services Engineer, CCMPA

GRAPHIC DESIGN

Natalia Leposavic, M.Arch.

COVER PAGE

Photo credit: Bill McEwen, P.Eng.
Graphic design: Marjorie Greene, AICP

Canadian Concrete Masonry Producers Association

P.O. Box 54503, 1771 Avenue Road
Toronto, ON M5M 4N5
Tel: (416) 495-7497
Fax: (416) 495-8939
Email: information@ccmpa.ca
Web site: www.ccmpa.ca

The Canadian Concrete Masonry Producers Association (CCMPA) is a non-profit association whose mission is to support and advance the common interests of its members in the manufacture, marketing, research, and application of concrete masonry products and structures. It represents the interests of Region 6 of the National Concrete Masonry Association (NCMA).

Contents Summary

Chapter 1	NBCC 2005 Seismic Provisions	
Objective: *to provide background on seismic response of structures and seismic analysis methods and explain key NBCC 2005 seismic provisions of relevance for masonry design*		**DETAILED NBCC SEISMIC PROVISIONS**

Chapter 2	Seismic Design of Masonry Walls to CSA S304.1	
Objective: *to provide background and commentary for CSA S304.1-04 seismic design provisions related to reinforced concrete masonry walls, and discuss the revisions in CSA S304.1-04 seismic design requirements with regard to the 1994 edition*		**DETAILED MASONRY DESIGN PROVISIONS**

Chapter 3	Summary of Changes in NBCC 2005 and CSA S304.1-04 Seismic Design Requirements for Masonry Buildings	
Objective: *to provide a summary of NBCC 2005 and CSA S304.1-04 changes with regard to previous editions (NBCC 1995 and CSA S304.1-94) and to present the results of a design case study of a hypothetical low-rise masonry building to illustrate differences in seismic forces and masonry design requirements due to different site locations and different editions of NBCC and CSA S304.1*		**SUMMARY OF NBCC AND S304.1 CHANGES**

Chapter 4	Design Examples	
Objective: *to provide illustrative design examples of seismic load calculation and distribution of forces to members according to NBCC 2005, and the seismic design of loadbearing and nonloadbearing masonry elements according to CSA S304.1-04*		**DESIGN EXAMPLES**

Appendix A	**Comparison of NBCC 1995 and NBCC 2005 Seismic Provisions**
Appendix B	**Research Studies and Code Background Relevant to Masonry Design**
Appendix C	**Relevant Design Background**
Appendix D	**Design Aids**
Appendix E	**Notation**

TABLE OF CONTENTS – APPENDIX A

A Comparison of NBCC 1995 and NBCC 2005 Seismic Provisions

This appendix provides a review of the NBCC 1995 seismic design provisions, and compares the base shear force and bending moments for a shear wall structure for both the 1995 and 2005 codes. It provides a means of assessing the changes in the seismic design provisions in the two codes, and is organized so that the sections in this appendix follow the same order as the sections in Section 1.5 of Chapter 1.

A.1 NBCC 1995 Seismic Hazard

Section 1.5.1, Chapter 1

4.1.9.1.6)

The seismic hazard in NBCC 1995 is given by the product $v \cdot S$, where S is a shape function shown in Figure A-1, and v is the zonal velocity ratio. The product $v \cdot S$ is very much like an acceleration response spectrum, as it provides a measure of hazard for different structural periods. The magnitude of v and the shape of S are based on estimates of the peak ground velocity and peak ground acceleration, for a 10% in 50 year probability of non-exceedance (1/475 per year probability). The v value is based directly on the peak ground velocity, while the shape of the S function is based on the ratio of the peak ground acceleration (expressed in terms of g) to the peak ground velocity (expressed in m/sec). For code purposes, these values are represented by the parameters Z_a and Z_v, which are used to define the seismic zones set out in the 1995 code. Eastern sites located on the Canadian Shield have high Z_a/Z_v ratios, because hard rock transmits high frequency waves more readily than does the soil and fractured rock of Western Canada, which generally has $Z_a/Z_v \leq 1$. The result is that the seismic hazard is dependent on two site parameters with a 1/475 per year probability.

Note that $v \cdot S$ does not represent the true seismic hazard as the long period values have been increased to account for higher mode effects in structures. S decreases as $1/\sqrt{T}$ in the longer period range, while $S_a(T)$ in NBCC 2005, which better represents a true spectrum, decreases much more rapidly (as a function of $1/T$ beyond 2 seconds). The higher mode effects in structures in NBCC 2005 are explicitly accounted for by use of the M_v factor.

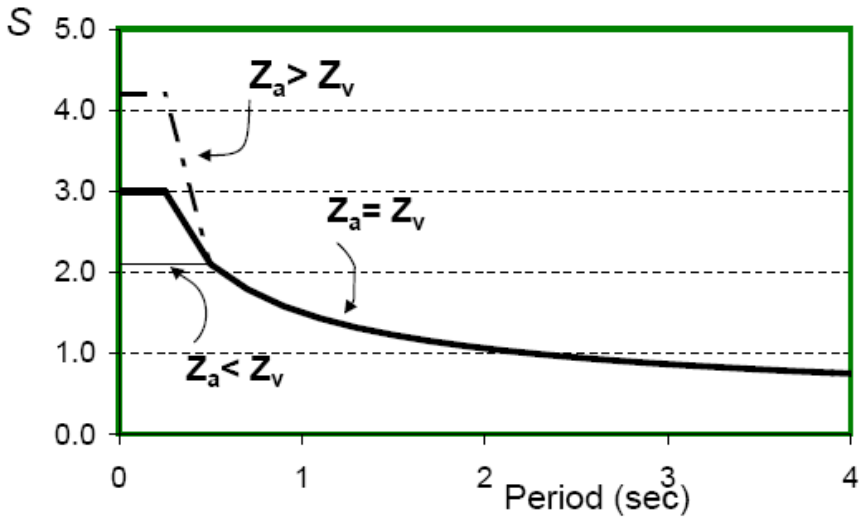

Figure A-1. S function according to NBCC 1995.

A.2 Effect of Site Soil Conditions

Section 1.5.2, Chapter 1

4.1.9.1.11)

The site soil amplification procedure in NBCC 1995 is considerably simpler that that in NBCC 2005. There is only one parameter that multiplies the S function, although there are limits on the amplification in the short period region for some sites.

F denotes the foundation factor which is given in Table A-1. It is applied as a multiplier to S, with the restriction that

$F \cdot S \leq 3.0$ where $Z_a \leq Z_v$, and

$F \cdot S \leq 4.2$ where $Z_a > Z_v$,

i.e., the foundation factor need not increase the short period end of the S function except when $Z_a < Z_v$.

Table A- 1. NBCC 1995 Foundation Factors

Foundation Factors		
Category	***Type and Depth of Soil Measured from the Foundation or Pile Cap Level***	F
1	Rock, dense and very dense coarse-grained soils, very stiff and hard fine-grained soils; compact coarse-grained soils and firm and stiff fine-grained soils from 0 to 15 m deep	1.0
2	Compact coarse-grained soils, firm and stiff fine-grained soils with a depth greater than 15 m; very loose and loose coarse-grained soils and very soft and soft fine-grained soils from 0 to 15 m deep	1.3
3	Very loose and loose coarse-grained soils with depth greater than 15 m	1.5
4	Very soft and fine-grained soils with depth greater than 15 m	2.0

A.3 Methods of Analysis

Section 1.5.3, Chapter 1

4.1.9.1.13.b)

NBCC 1995 does not prescribe a specific method of seismic analysis for building structures. However, Cl.4.1.9.1.13.b) related to vertical force distribution, states that the total lateral seismic force V shall be distributed by means of an equivalent static analysis procedure (part a), or by dynamic analysis with the seismic effects scaled so that the base shear from the dynamic analysis equals V (part b). Commentary J to the NBCC 1995 (NRC, 1996) states that the application of dynamic analysis pertains "especially to buildings with significant irregularities either in plan or elevation, and buildings with setbacks or major discontinuities in stiffness or mass. Performing a dynamic analysis will lead to a better representation of modal contribution in tall buildings."

A.4 Base Shear Calculations

Section 1.5.4, Chapter 1

4.1.9.1.4)

The formula for the design base shear V according to the NBCC 1995 is:

$$V = \left(\frac{V_e}{R} \right) U$$

where

$V_e = v \cdot S \cdot I \cdot F \cdot W$

represents the elastic shear force.

The design parameters used in the NBCC 1995 base shear equation are explained in Table A-2. A comparison of V between the 1995 and 2005 codes is presented in Section A.12.

NBCC 1995 (Cl.4.1.9.1.7) prescribes the following relations for the fundamental period T of wall structures:

a) $T = 0.09 h_n \sqrt{D_s}$

where

h_n (m) is building height from the base i.e. top of foundations to the roof level,

D_s (m) is the length of wall or braced frame which constitutes the main lateral load-resisting system in a direction parallel to the applied forces. When the length of the lateral load resisting system is not well defined, then the Code requires that D, the length of building in the direction parallel to the applied forces, shall be used instead of D_s.

b) other established methods of mechanics; with the restriction that the value of V_e used for design shall be not less than 0.80 of the value computed using the period calculated in a).

The period given by the formula (a), which is based on measured values, is a conservative (low) estimate from the data, and generally is smaller than that found using method (b), particularly if the length D is used in the calculation. The code adopted this

low estimate as it leads to higher, more conservative, forces. The limit prescribed in (b) is applied to the base shear and not to the period, as the base shear is very sensitive to period in some areas.

Table A- 2. NBCC 1995 Seismic Design Parameters

v =	zonal velocity ratio for the site from the climatic data table in Appendix C of NBCC 1995, based on ground motion associated with a 10% probability of exceedance in 50 years (475 year earthquake).
S =	the seismic response factor, dependent on the Z_a/Z_v ratio for the site and the period T of the structure (see Section A.1).
I =	Importance factor for the structure, equal to I=1.5 for "post-disaster" structures, 1.3 for schools, and 1.0 for ordinary structures;
F =	Foundation factor related to soil conditions (see Section A.2 and Table A-1)
W =	dead weight plus some portion of live load that would move laterally with the structure. Live loads considered are 25% of the snow load, 60% of storage loads for areas used for storage, and the full contents of any tanks. 100% of the live loads are not used as the probability of that occurring at the same time as the earthquake is small. Also, live loads such as people or cars would not move with the same motion as the building.
R =	force modification factor that represents the capability of a structure to dissipate energy through cyclic inelastic (ductile) behaviour. For masonry structures designed and detailed according to CSA S304.1-94: *R* = 2.0 for reinforced walls with nominal ductility, 1.5 for regular reinforced masonry and 1.0 for unreinforced masonry.
U =	0.60, and is described as a "factor representing level of protection based on experience". U was introduced so as to make the design base shear for the 1995 code similar to that in previous codes. Some persons later thought of U as being an overstrength factor, recognizing that the structure has strength higher than the nominal yield strength, but this was not the basis for the introduction of U .

A.5 Force Reduction Factor R

Section 1.5.5, Chapter 1

4.1.9.1.8)

NBCC 1995 had only one R factor, equivalent to the R_d factor in NBCC 2005. NBCC 1995 Table 4.1.9.1.B allows $R = 2$ for reinforced masonry with nominal ductility, $R = 1.5$ for regular reinforced masonry, and $R = 1$ for unreinforced masonry. These values are equivalent to walls with moderate ductility, conventional construction and unreinforced masonry, respectively, in NBCC 2005. Height limitations, and some other provisions that required reinforced masonry, were given in Clause 4.1.9.3 Special Provisions NBCC 1995.

A.6 Higher Mode Effects

Section 1.5.6, Chapter 1

NBCC 1995 does not explicitly mention higher mode effects in calculating the base shear *V*, but the *S* function has been set artificially high in the long period region to account for the contribution from the higher modes. Higher mode effects are considered

in the distribution of forces along the height of the structure, see Section A.7, and in calculating the overturning moments, Section A.8.

Note that in contrast to NBCC 2005, the higher mode effects in the 1995 code make no distinction between walls or frames.

A.7 Vertical Distribution of Seismic Forces

Section 1.5.7, Chapter 1

4.1.9.1.13.a)

The distribution of the inertial forces to the floors in NBCC 1995 is essentially the same as in NBCC 2005, and is summarized below

$$F_x = \left(V - F_t\right) \cdot \frac{W_x h_x}{\sum_{i=1}^{n} W_i h_i}$$

where
F_x – seismic force acting at level x
W_x - portion of W that is assigned to level x
h_x – height from the base of the structure up to the level x
F_t – a portion of the base shear to be applied as an additional force to F_n at the top of the building, and is given by

$F_t = 0$ for T_a < 0.7 sec

$F_t = 0.07 T_a V$ for 0.7 < T_a < 3.6 sec

$F_t = 0.25 V$ for T_a > 3.6 sec

where T_a is the fundamental lateral period.

Once the forces at each floor are established, the total storey shears can simply be calculated using statics.

A.8 Overturning Moments (J factor)

Section 1.5.8, Chapter 1

4.1.9.1.23-27

In NBCC 1995, the overturning moment, M , at the base of the structure, shall be reduced by the factor J , where

$J = 1$ for $T < 0.5s$
$J = 1 - 0.2T$ for $0.5s < T < 1.5s$
$J = 0.8$ for $T > 1.5s$

The overturning moment M_x at any level x shall be multiplied by J_x, where

$J_x = J + (1 - J)(h_x / h_n)^3$

where h_n is the height to the top of the structure.

Unlike NBCC 2005, the J factor in NBCC 1995 is not dependent on the structure type or the site conditions.

A.9 Torsion

Section 1.5.9, Chapter 1

4.1.9.1.28)

At each storey level throughout the building, the torsional moment applied is taken as one of the following four cases:

i) $T_x = F_x\left(1.5e_x + 0.1D_{nx}\right)$

ii) $T_x = F_x\left(1.5e_x - 0.1D_{nx}\right)$

iii) $T_x = F_x\left(0.5e_x + 0.1D_{nx}\right)$

iv) $T_x = F_x\left(0.5e_x - 0.1D_{nx}\right)$

where

F_x is lateral force at the x^{th} floor level,

e_x is the eccentricity at level x, and is distance between the centre of mass and the centre of rigidity in the direction perpendicular to the direction of F_x, and

D_{nx} is a plan dimension of the building at level x perpendicular to the direction of F_x.

Note that $0.1D_{nx}$ is termed the accidental eccentricity.

Each element in the building must be designed for the most severe effect of the above load cases.

Note that it is necessary to explicitly determine the value of e_x. However, if a static 3-D structural analysis program is available, it is possible to use a combination of two analyses to determine $F_x\left(1.5e_x\right)$ and $F_x\left(0.5e_x\right)$ without explicitly determining the e_x.

Alternately, if a 3-D dynamic analysis is carried out the effects of accidental eccentricity should be accounted for by combining the dynamic analysis element forces with the results from a static analysis of either of the two cases of accidental torques given by:

$T_x = +F_x\left(0.1D_{nx}\right)$, or

$T_x = -F_x\left(0.1D_{nx}\right)$

In all of the above analyses, F_x represents the storey force from the static analysis described earlier.

A.10 Irregularities and Restrictions

Section 1.5.10, Chapter 1

4.1.9.3)

NBCC 1995 has very few restrictions regarding irregularities. Masonry is specifically mentioned as requiring reinforcement if Z_a or Z_v is 2 or higher, but there are no height limitations based on irregularities as found in NBCC 2005.

A.11 Displacements

Section 1.5.11, Chapter 1

4.1.9.2.1-3)

In NBCC 1995, displacements are to be calculated using the reduced design forces as given by *V*, and then multiplied by *R* to give realistic values. Since *V* is given by

$$V = \left(\frac{V_e}{R} \right) U \ ,$$

this would imply that the displacements are the elastic displacements reduced by the factor *U*, which has been a somewhat controversial issue. One difference in the codes, is that V_e in the 1995 code is multiplied by the importance factor *I*, while in NBCC 2005 the displacements are not dependent on the importance factor.

The drift ratio limits in NBCC 1995 are 0*.01 for post-disaster buildings* and *0.02 for all other structures*. This is essentially the same as NBCC 2005, except for ordinary structures which can have a drift ratio of 0.025. Overall, the drift limits in NBCC 2005 are tighter than in the 1995 code.

A.12 Shear and Moment Comparison

This section provides a comparison of the base shear and base moment for ductile masonry walls under the NBCC 1995 and NBCC 2005 codes, for periods ranging from very short to four seconds. For ductile masonry shear walls, Toronto and Vancouver have been selected to investigate the effect of the different spectral shapes between eastern and western Canada.

Figure A-2a shows the shear comparison for a site in Toronto, and Figure A-2b for Vancouver. It is assumed that both sites are on firm ground with no soil amplification (site Class C per NBCC 2005). The following force modification factors were used:
R=2 and *U=0.6* for the NBCC 1995 code calculation, and
R_d*=2* and R_o*=1.5* for the NBCC 2005 values

In each plot, the line titled 'NBC 2005 spectral shape' represents the *V/W* ratio for the 2005 code, for the same values of R_d and R_o used in the design calculations, but without considering the upper and lower bounds on *V* per NBCC 2005, and with M_v=1 for all periods.

The comparison for Toronto in Figure A-2a shows that there is not much difference in the design level base shear between the codes, with the 2005 code values being lower in the short and long period ranges, but higher for intermediate periods. At a period of 2 seconds, the M_v value is equal to 2.5 for Toronto. The effect of this in increasing the shear is very apparent at the longer periods when compared to the NBCC 2005 spectral shape. Also, it is apparent that without the short period cutoff, the short period shears from NBCC 2005 would be much larger than the NBCC 1995 values.

The comparison for Vancouver in Figure A-2b shows that the NBCC 2005 design base shear is larger than the NBCC 1995 base shear over the entire period range, especially around 0.5 seconds. The M_v factor for Vancouver is equal to 1.2 at the period of 2 seconds, and so has little effect on the long period base shear.

In general, it appears that the base shear from NBCC 2005 is larger than that from NBCC1995. However, because the periods given by the two codes may be different, and because the limit placed on using a longer calculated period is more liberal in the short period end in NBCC 2005, it may be that in some cases there may be a smaller difference in design base shear than the figures indicate.

Since wall size and reinforcement are mainly governed by the wall moments, a moment comparison of the two codes may be more meaningful than a shear comparison.

Figure A-3 compares the base bending moment for NBCC 1995 and NBCC 2005 for the same cases as shown in Figure A-2. The units are not particularly meaningful, but allow a comparison to be made between the two codes. In the short period range less than 1.0 seconds, the moment comparisons are essentially the same as the shear comparisons. But for longer periods, particularly for Toronto, the small value of J at periods of 2.0 s and greater for NBCC 2005 substantially reduces the moments, resulting in much smaller design moments at the longer periods compared to the NBCC 1995 code, as shown in Figure A-3a. For Vancouver, the J factor is larger and does not have as much an effect, but it does bring the design moments from the two codes into close agreement in the longer periods.

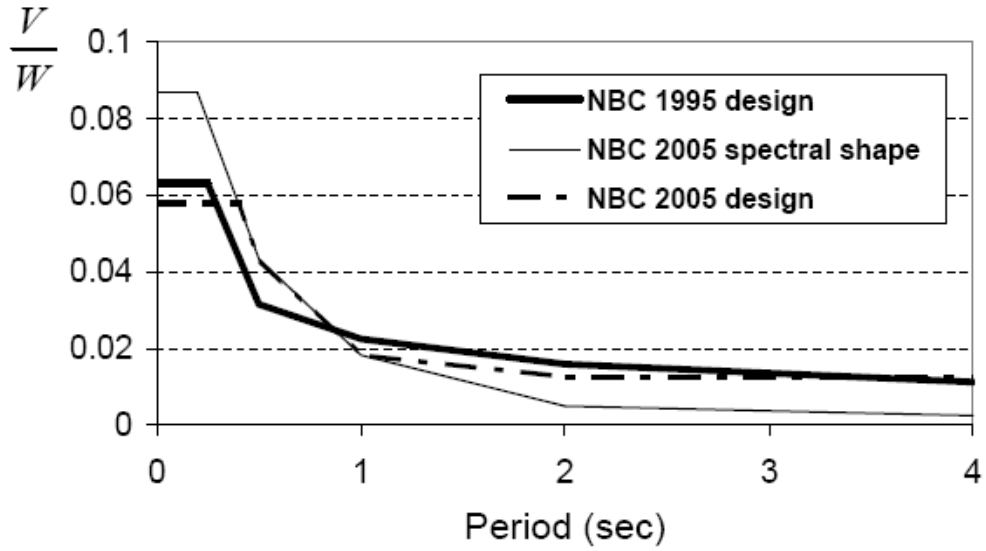

a)

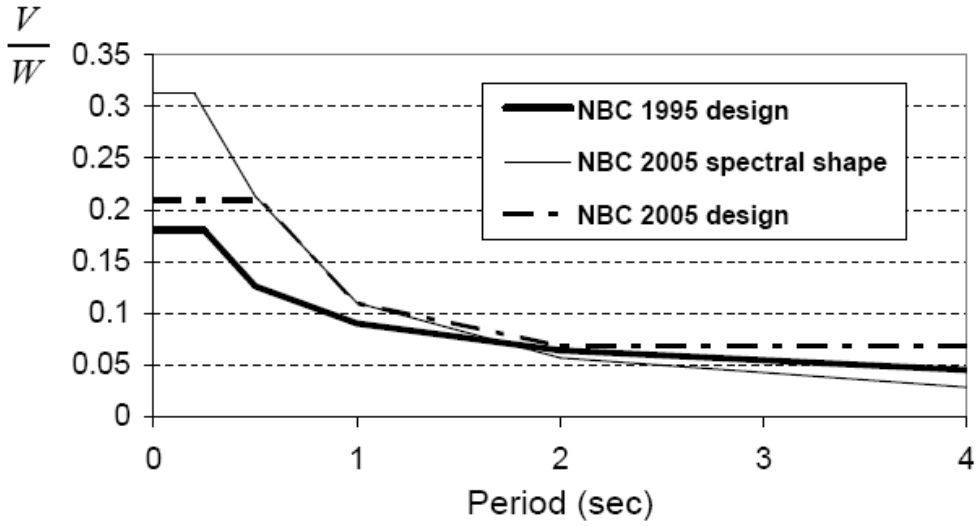

b)

Figure A-2. Base shear comparison for NBCC 1995 and NBCC 2005: a) Toronto; b) Vancouver.

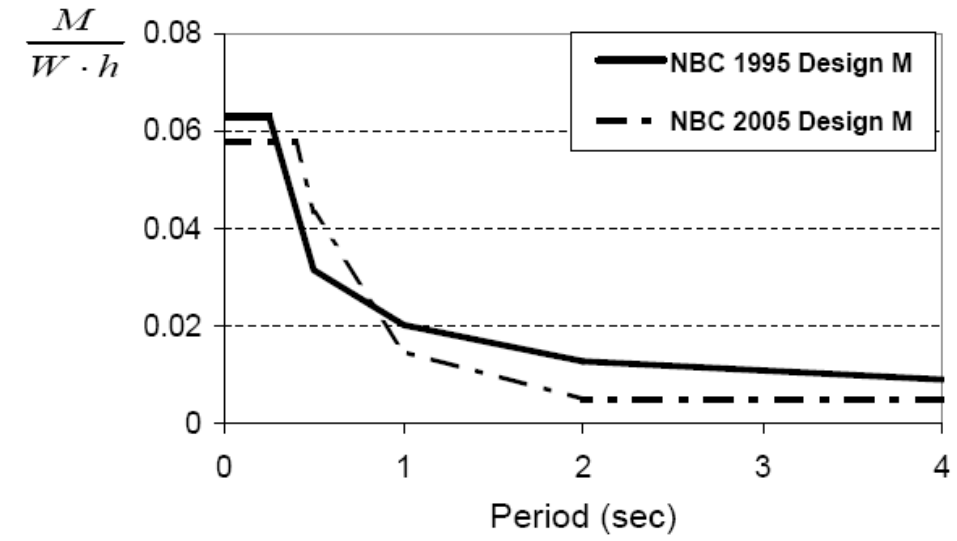

a)

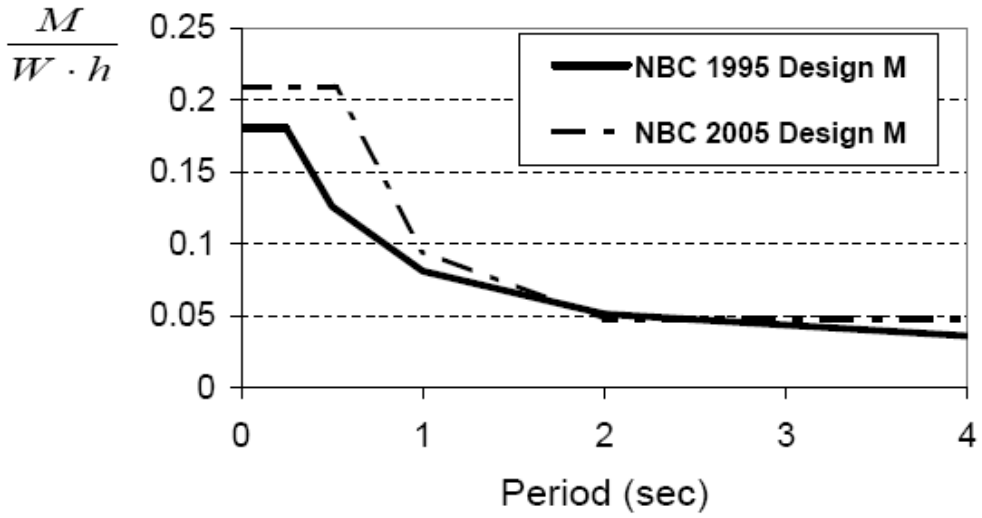

b)

Figure A-3. Base bending moment comparison for NBCC 1995 and NBCC 2005: a) Toronto; b) Vancouver.

TABLE OF CONTENTS – APPENDIX B

B Research Studies and Code Background Relevant to Masonry Design

This appendix contains additional background material relevant to the aspects of masonry design discussed in Chapter 2. Findings of some relevant research studies, as well as the discussion on provisions of masonry design codes from other countries, are included. This information may be useful to readers interested in gaining a more detailed insight into the subject. However, it should be noted that designers may use alternative design provisions in situations where CSA S304.1 is silent on a specific issue. The design provisions contained in design standards from other countries cannot supersede the provisions of pertinent Canadian standards.

B.1 Shear/Diagonal Tension Resistance

Axial compression:

An experimental study on reinforced masonry wall specimens by Voon and Ingham (2006) showed that an increase in axial compression stress from 0 to 0.5 MPa resulted in an increase in the maximum wall shear resistance of more than 20%. However, walls subjected to higher axial compression had a reduced post-cracking deformation capacity, resulting in a more brittle failure pattern. The presence of higher axial stress also delayed the onset of diagonal cracking in the walls from the lateral loads, as the vertical stress reduced the principal stress that leads to cracking.

The latest edition of New Zealand Masonry Standard NZS 4230:2004 (SANZ, 2004) prescribes a different method for calculating the axial load contribution to masonry shear resistance than CSA S304.1-04 for low aspect walls. This contribution (equal to $0.9N\tan\alpha$), results from a diagonal strut mechanism, which is based on an assumption that axial compression load N must effectively form a compression strut at an angle α to the axis (see Figure B-1). The axial load must be transmitted through the flexural compression zone, while the horizontal component of the strut force resists the applied shear force (Priestley et al., 1994). This model implies that the shear strength of squat walls under axial loads should be greater than that of more slender walls, and higher than that prescribed in CSA S304.1-04. According to this model, the axial load contribution is limited to $N \le 0.1 f'_m A_g$.

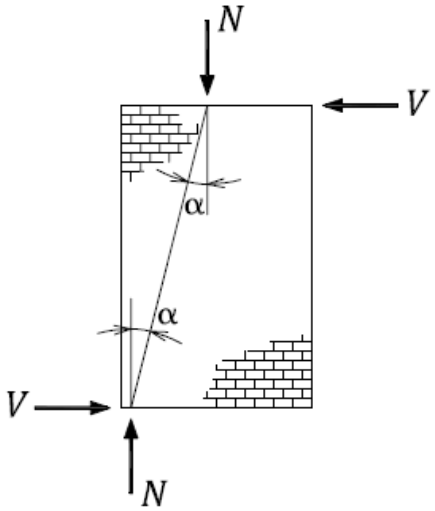

Figure B-1. Contribution of axial load to wall shear strength (reproduced from NZS 4230:2004 with the permission of Standards New Zealand under Licence 000725).

Grouting pattern:
Experimental studies have reported a significant reduction in shear resistance for partially grouted walls compared to otherwise identical fully grouted walls, however partially grouted masonry is a viable lateral load resisting system for regions of low to moderate seismic risk. Schultz (1996) tested a series of six partially grouted reinforced block wall specimens under in-plane cyclic loads. Only the outermost vertical cores and a single course bond beam at midheight were grouted. The mechanism of shear resistance in partially grouted walls is characterized by the development of vertical cracks between ungrouted and grouted masonry due to stress concentrations or planes of weakness (this mechanism is different than the one expected to develop in solidly grouted masonry walls). It was also reported that an increase in horizontal reinforcement ratio did not have a significant effect on the overall shear resistance.

An experimental study by Voon and Ingham (2006) showed that the shear strength of a solidly grouted wall specimen was approximately 110% higher than an otherwise identical specimen with 30% grouted cores. Also, the specimen with 55% grouted cores had more than a 50% higher shear strength compared to the specimen with 30% grouted cores. However, the difference is smaller when the shear stress is compared using the net wall area.

Wall aspect ratio:
The findings of several experimental studies, e.g. Matsumura (1987), Okamoto et al. (1987), and Voon (2007) confirmed that masonry walls with lower aspect ratios exhibited shear strengths that were larger than those for more slender masonry walls. The researchers concluded that the shear strength enhancement was due to the more prominent role of arching action in masonry walls with low aspect ratios, in which shear was mainly resisted by compression struts (see Figure 2-16a).Voon and Ingham (2006) reported that the shear resistance decreased by 15% when the wall aspect ratio increased from 1.0 to 2.0. A squat wall specimen with an aspect ratio of approximately 0.6 showed a significant increase in shear resistance (by over 100%) as compared to a specimen with aspect ratio of 1.0. The findings of an experimental study by Okamoto et al. (1987) confirmed that the wall shear strength increased by 20 to 30% when the aspect ratio decreased from 2.3 to 1.6 and from 2.3 to 0.9 respectively. A study of partially grouted masonry block walls by Schultz (1996) showed that a decrease in the wall aspect ratio was reported to have a beneficial effect on the shear resistance, that is, squat walls are expected to have larger shear resistance than flexural walls of the same height. However, squat wall specimens also showed a reduced deformation capacity and increased strength deterioration.

Steel shear resistance V_s:
Shear reinforcement in masonry walls does not seem to be as effective as in concrete walls. A possible explanation is that the reinforcing bars located where the inclined crack crosses near the end of the bar are unable to develop their full yield strength in the masonry walls. To account for this phenomenon, the New Zealand Masonry Standard NZS 4230:2004 (SANZ, 2004) prescribes a coefficient of 0.8 in the V_s equation, while CSA S304.1-04 uses a 0.6 factor. This phenomenon is particularly pronounced in short walls where it is likely that the length of the shear reinforcement is insufficient to fully develop its yield strength.

It should be acknowledged that horizontal reinforcement in masonry walls usually does not have as good anchorage as the corresponding reinforcement in concrete walls. Anderson and Priestley (1992) have noticed that straight bars or 90° hooks were used in some experimental studies (see Figure B-2a), whereas the horizontal reinforcement in concrete walls is usually anchored in a more effective way, that is, by means of 180° hooks. The type and extent of anchorage are expected to influence the effectiveness of shear reinforcement. Anderson and

Priestley also found that shear strength didn't show any correlation with the vertical reinforcement ratio.

According to some researchers (Shing et al., 1990; Tomazevic, 1999; Voon, 2007), a fraction of the wall shear resistance can be attributed to the presence of vertical reinforcement. Dowel action in vertical reinforcing bars enables shear transfer across a diagonal crack by the localized kinking in reinforcing bars due to their relative displacement (see Figure B-2b) (note that compression kinks cancel out some of the tension kinks). However, once the vertical reinforcement yields, as it would in the plastic hinge zone of ductile walls, its contribution to the shear resistance drops significantly, so CSA S304.1 ignores its contribution to the wall shear resistance.

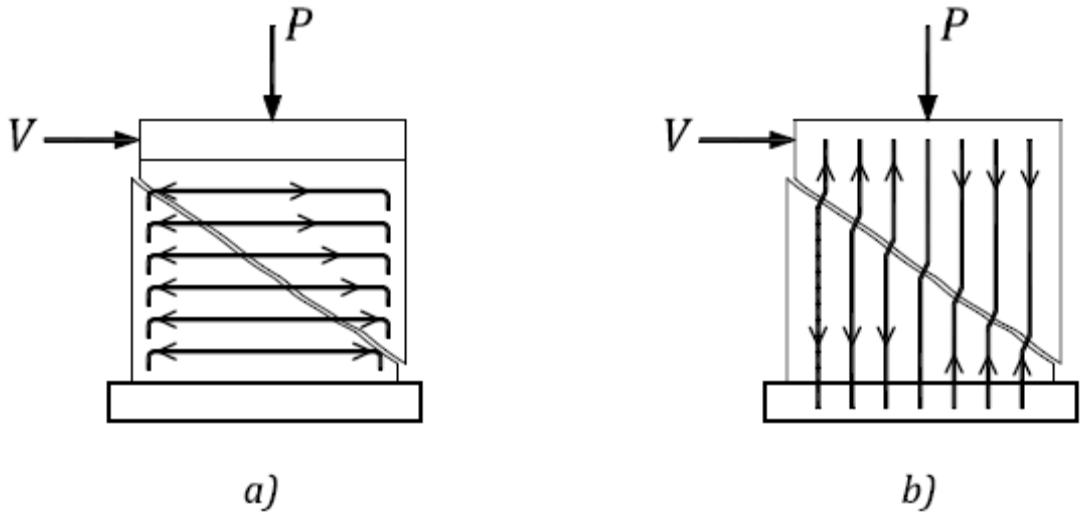

Figure B-2. Wall reinforcement contributing to shear resistance: a) horizontal reinforcement acting in tension; b) dowel action in vertical reinforcement (Tomazevic, 1999, reproduced by permission of the Imperial College Press).

B.2 Ductile Seismic Response

A prime consideration in seismic design is the need to have a structure that is capable of deforming in a ductile manner when subjected to several cycles of lateral loading well into the inelastic range. This section explains a few key terms related to ductile seismic response, including ductility ratio, curvature, plastic hinge, etc. It is very important for a structural designer to have a good understanding of these concepts before proceeding with the seismic design and detailing of ductile masonry walls according to CSA S304.1.

Ductility is a measure of the capacity of a structure or a member to undergo deformation beyond yield level, while maintaining most of its load-carrying capacity. Ductile structural members are able to absorb and dissipate earthquake energy by inelastic (plastic) deformations that are usually associated with permanent structural damage. These inelastic deformations are concentrated mainly in regions called *plastic hinges*. In general, plastic hinges develop in shear walls responding in the flexural mode and are typically formed at their base. An example of a plastic hinge formed in a reinforced masonry wall subjected to seismic loading is shown in Figure 2-8a. The concept of ductility and ductile seismic response was introduced in Section 1.4.3.

A common way to quantify ductility in a structure is through the *displacement ductility ratio* μ_Δ. This is the ratio of the maximum lateral displacement experienced by the structure at the ultimate (Δ_u), to the displacement at the onset of inelastic response (Δ_y) (see Figure 1-5c).

$$\mu_\Delta = \frac{\Delta_u}{\Delta_y}$$

Next, the concept of curvature will be explained by an example of a reinforced masonry shear wall subjected to bending due to a shear force applied at the top, as shown in Figure B-3a. Consider a wall segment ABCD of unit height. This segment deforms due to bending moments, so sections AB and CD rotate by a certain angle relative to their original horizontal position (these deformed sections are denoted as A'B' and C'D'). Rotation between the ends of the segment defines the curvature φ, as shown in Figure B-3b. Curvature represents relative section rotations per unit length. It should be noted that curvature is directly proportional to the bending moment at the wall section under consideration, if the section remains elastic.

Consider any section CD that undergoes curvature φ, as shown in Figure B-3c. Strain distribution along the wall section is defined by the product of curvature and the distance from the neutral axis, located by the depth c. The maximum compressive strain in masonry ε_m is given by

$$\varepsilon_m = \varphi \cdot c$$

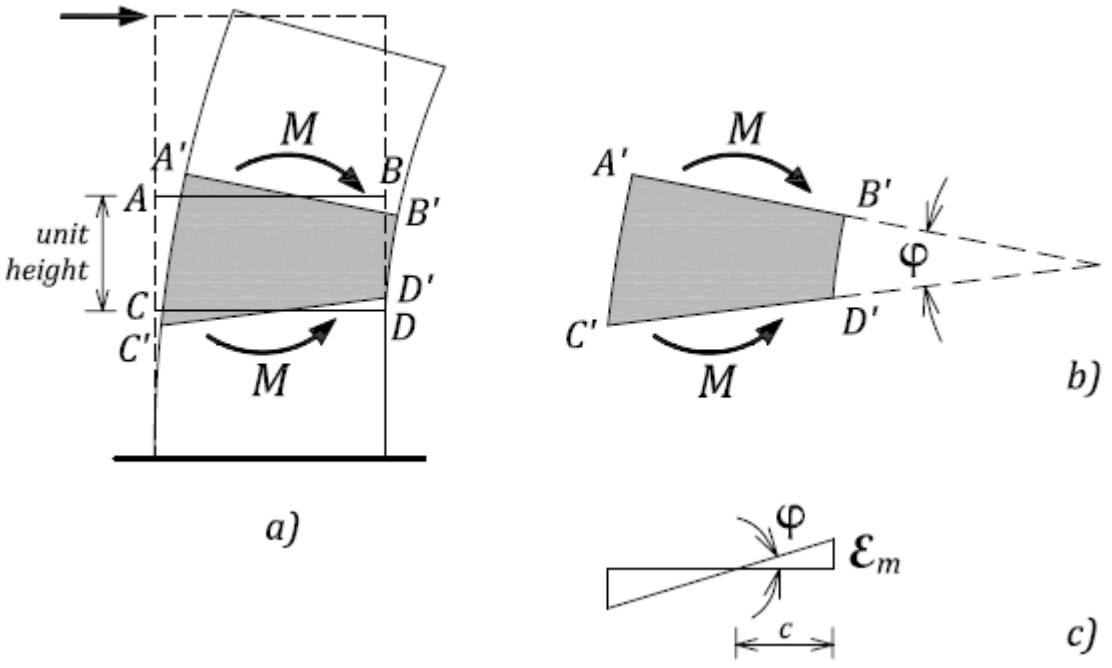

Figure B-3. Curvature in a shear wall subjected to flexure: a) wall elevation; b) deformed wall segment ABCD; c) strain distribution along the section CD.

For the seismic design of reinforced masonry walls, it is of interest to determine curvatures at the following two stages: the onset of steel yielding and at the ultimate stage. Consider a reinforced masonry wall section subjected to axial load and bending shown in Figure B-4a.

Yield curvature φ_y corresponds to the onset of yielding characterized by tensile yield strain ε_y developed in the end rebars, as shown in Figure B-4b, where

$$\varphi_y = \frac{\varepsilon_y}{l_w - d' - c}$$

Ultimate curvature φ_u corresponds to the ultimate stage, when the maximum masonry compressive strain ε_m has been reached. The maximum ε_m value has been limited to 0.0025 by CSA S304.1-04 (see Figure B-4c) to prevent damage to the outer blocks in the plastic hinge region. Note that the neutral axis depth c is going to decrease as more of the reinforcement has yielded (see Figure B-4c).

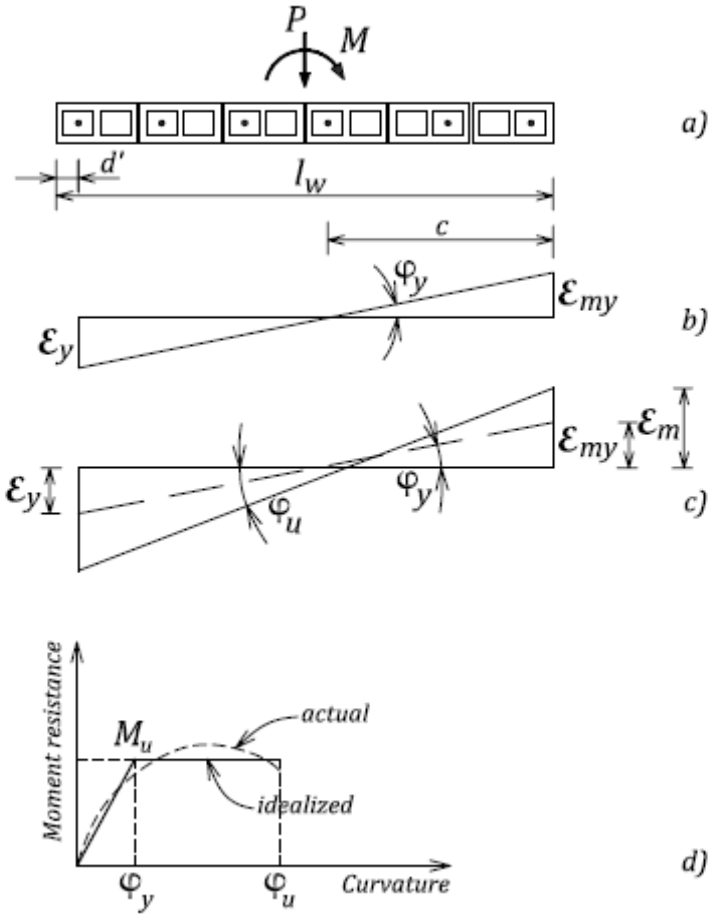

Figure B-4. Curvature in a reinforced masonry wall section: a) wall cross section; b) yield curvature; c) ultimate curvature; d) moment-curvature relationship.

The curvature value depends on the load level, the section geometry, the amount and distribution of reinforcement, and the mechanical properties of steel and masonry. An actual moment-curvature relationship for ductile sections is nonlinear, however it is usually idealized by elastic-plastic (bilinear) relationship, as shown in Figure B-4d.

Once the curvatures at the critical stages have been determined, the *curvature ductility ratio* μ_φ can be found as follows

$$\mu_{\varphi} = \frac{\varphi_u}{\varphi_y}$$

When the curvature distribution along a structural member (e.g. shear wall) is defined, rotations and deflections can be calculated by integrating the curvatures along the member. This can be accomplished in several ways, including the moment area method.

Rotations and deflections in a masonry shear wall at the ultimate state can be determined following the approach outlined above. Consider a cantilevered shear wall of length l_w and height h_w, and the plastic hinge length l_p (see Figure B-5a). The wall is subjected to a seismic shear force at the top, which results in a corresponding bending moment diagram as shown in Figure B-5b. The curvature diagram shown in Figure B-5c has two distinct portions: an elastic portion, with the maximum curvature equal to the yield curvature φ_y, and the plastic portion with the maximum curvature equal to the ultimate curvature φ_u. Note that the elastic portion of the curvature diagram has the same shape as the bending moment diagram (since the curvatures and bending moments are directly proportional). The actual curvature distribution in the plastic region varies in a nonlinear manner, as shown in Figure B-5c. For design purposes, the curvature can be taken as constant over the plastic hinge length l_p (note that the areas under the actual and the equivalent plastic curvature are set to be equal). The elastic rotation θ_e and the plastic rotation θ_p are presented in Figure B-5d. The plastic rotation can be determined as the area of the equivalent rectangle of width $\varphi_u - \varphi_y$ and height l_p, as shown in Figure B-5c. These rotations can be calculated from the curvature diagram as follows:

$$\theta_u = \theta_e + \theta_p$$

where

$$\theta_e = \frac{\varphi_y \cdot h_w}{2}$$

$$\theta_p = \left(\varphi_u - \varphi_y\right) \cdot l_p$$

The maximum deflection Δ_u at the top of the wall is shown in Figure B-5d. This deflection has two components: elastic deflection Δ_y corresponding to the yield curvature φ_y, and the plastic deflection Δ_p due to a rigid body rotation, since bending moments do not increase once the yielding has taken place. Deflection values can be found by taking the moment of the curvature area around point A, as follows:

$$\Delta_y = \frac{\varphi_y h_w}{2} \cdot \frac{2h_w}{3} = \frac{\varphi_y h_w^{\,2}}{3}$$

$$\Delta_p = \left(\varphi_u - \varphi_y\right) \cdot l_p \left(h_w - 0.5 l_p\right)$$

$$\Delta_u = \Delta_y + \Delta_p$$

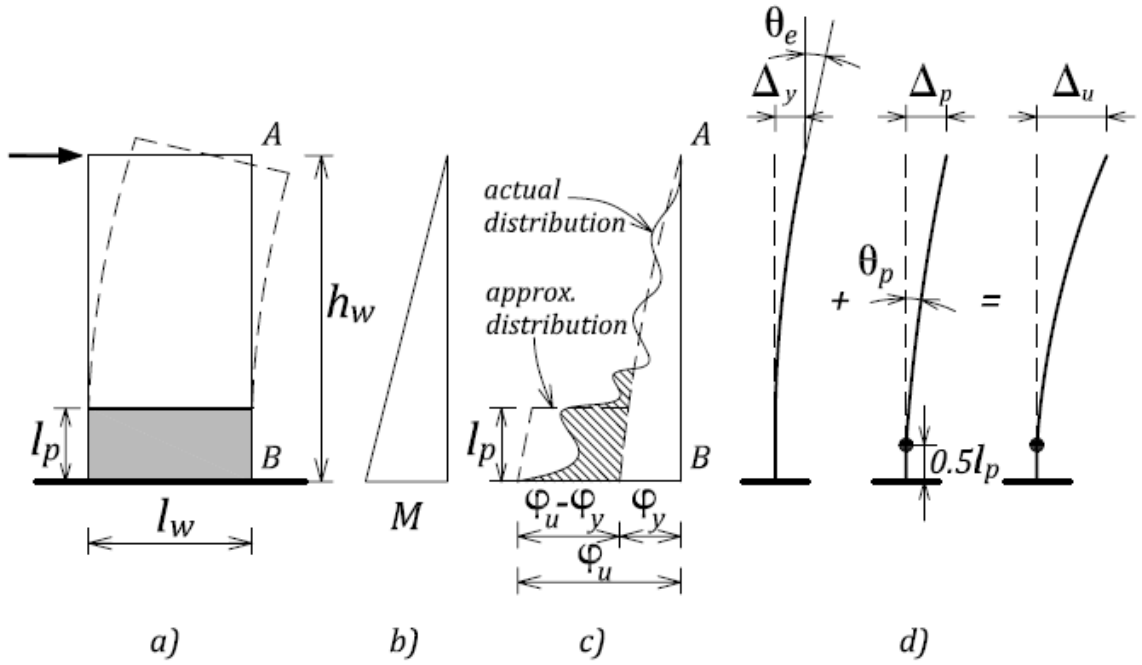

Figure B-5. Shear wall at the ultimate: a) wall elevation; b) bending moment diagram; c) curvature diagram; d) deflections.

The above equations can be used to determine the displacement ductility ratio μ_Δ, in terms of the curvature ductility μ_φ and other parameters, as follows:

$$\mu_\Delta = \frac{\Delta_u}{\Delta_y} = 1 + 3(\mu_\varphi - 1)\left(\frac{l_p}{h_w}\right)\left(1 - 0.5\frac{l_p}{h_w}\right)$$

Alternatively, the curvature ductility ratio μ_φ can be expressed in terms of the displacement ductility ratio, as follows:

$$\mu_\varphi = \frac{\varphi_u}{\varphi_y} = \frac{h_w^{\,2}(\mu_\Delta - 1)}{3l_p(h_w - 0.5l_p)} + 1$$

It should be noted that μ_Δ and μ_φ values are different for the same member. Once the yielding has taken place, the deformations concentrate at the plastic hinges, so the curvature ductility μ_φ is expected to be larger than the displacement ductility μ_Δ. This difference is more pronounced in walls with larger displacement ductility ratios.

B.3 Ductility Check

CSA S304.1-04 prescribes ductility check for certain classes of ductile masonry shear walls, as discussed in Section 2.5.4.3 of this document. Masonry design standards in other countries also contain ductility check provisions. For example, the New Zealand Masonry Standard NZS 4230:2004 (SANZ, 2004) Cl. 7.4.6 prescribes the c/l_w limit of 0.2 for limited ductile cantilever walls (provided that $h_w/l_w < 3$). The same limit was prescribed by the 1994 version of CSA S304.1. (Note that limited ductility walls according to the NZS 4230 are characterized by the displacement ductility of 2.0). It should be noted that the NZS 4230 prescribes maximum strain limits for unconfined and confined masonry of 0.003 and 0.008 respectively. The standard also

includes a provision for confining plates in plastic hinge regions as a means of confining the compression zone of the wall section and enhancing its ductile performance (NZS 4230:2004 Cl.7.4.6.5). The seismic design provisions for reinforced concrete shear walls in CSA A23.3-04 also prescribe c/l_w limits for shear walls at different ductility levels.

B.4 Wall Height-to-Thickness Ratio Restrictions

Paulay and Priestley (1992, 1993) developed an analytical model, which offers a means to find the minimum wall thickness required to avoid out-of-plane instability. This thickness depends on several parameters, including the vertical reinforcement ratio, desired curvature and displacement ductility ratios, plastic hinge length, and the mechanical properties of steel and masonry. Paulay and Priestley also performed an experimental study to confirm their analytical model. They tested a few reinforced concrete shear wall specimens and a concrete masonry wall specimen. The masonry wall specimen failed by out-of-plane buckling at a very large displacement ductility μ_Δ of around 14.

The application of this procedure will be illustrated on an example of a reinforced masonry wall. The equation for the critical wall thickness b_c is as follows (Paulay and Priestley, 1992)

$$b_c = 0.022 l_w \sqrt{\mu_\varphi}$$

Curvature ductility, μ_φ, is related to displacement ductility, μ_Δ, as shown in Section B.3. The plastic hinge length l_p is taken equal to $h_w/6$, and so the equation can be simplified as follows

$$\mu_\varphi = 2.2(\mu_\Delta - 1)$$

The displacement ductility ratio μ_Δ can be considered equal to R_d prescribed by NBCC 2005 for different SFRSs (note that μ_Δ values in the range from 2.0 to 3.0 are considered in this example). By following the above procedure, it is possible to obtain the b_c/l_w ratios corresponding to different μ_Δ values. The results are summarized in Table B-1.

For example, if the wall length l_w is equal to 5,000 mm, the corresponding critical thickness b_c is equal to 150 mm for μ_Δ = 2.0, or 230 mm for μ_Δ = 3.0. Paulay and Priestley suggest that the critical wall thickness should be expressed as a fraction of the wall length rather than its height.

Table B-1. Critical Wall Thickness b_c Versus the Displacement Ductility Ratio μ_Δ

μ_Δ	μ_φ	l_w/b_c
2.0	2.2	31
2.5	3.3	25
3.0	4.4	22

Findings of this research were incorporated in the seismic design provisions for reinforced concrete shear walls in New Zealand and Canada (CSA A23.3 first introduced these provisions in its 1994 edition). The New Zealand masonry design standard (NZS 4230:2004) also includes provisions, which restrict the thickness of reinforced masonry shear walls; however these provisions are somewhat less stringent than the current Canadian provisions. NZS 4230:2004 prescribes the following minimum thicknesses for limited ductility walls (μ_Δ of 2.0) and ductile walls (μ_Δ of 4.0):

1. For *walls up to 3 storeys high* (Cl.7.4.4.1 and 7.3.3), minimum thickness t should not be less than $L_n/20$ (or $0.05L_n$), where L_n denotes clear vertical distance between lines of effective horizontal support or clear horizontal distance between lines of effective vertical

support. Commentary to Cl.7.3.3 states that "for a given wall thickness, t, and the case when lines of horizontal support have a clear vertical spacing of $L_n > 20t$, then vertical lines of support having a clear horizontal spacing of $L_n < 20t$ shall be provided."

2. For *walls more than 3 storeys high* (Cl.7.4.4.1) minimum thickness t shall not be less than $L_n/13.3$ (or $0.075L_n$). However, a larger wall thickness can be used provided that one of the following conditions is satisfied (maximum strain in masonry ε_u is equal to 0.003 according to NZS 4230:2004) (see Figure 2-28):
    a) $c \le 4t$ or
    b) $c \le 0.3l_w$ or
    c) $c \le 6t$ from the inside of a wall return of a flanged wall, which has a minimum length $0.2L_n$.

The relaxed thickness requirement applies to the cases where the neutral axis depth is small, and so the compressed area may be so small that the adjacent vertical strips of the wall will be able to stabilize it. This is likely the case with rectangular walls subjected to low axial compression. (The same criteria for relaxed thickness restrictions are included in the seismic provisions for reinforced concrete design CSA A23.3-04 Cl.21.6.3.)

Commentary to NZS 4230 Cl.7.4.4.1 states that it is considered unlikely that failure due to lateral instability of the wall will occur in structures less than 3 storeys high, because of the rapid reduction in flexural compression with height. This is also in line with the statement made by Paulay (1986), that out-of-plane stability is likely to take place in walls with large plastic hinge length (one storey or more). According to CSA S304.1 Cl.10.16, plastic hinge length is related to the wall height (on the order of $h_w/6$), and so a large plastic hinge length would not be expected in shear walls found in low-rise masonry buildings.

Paulay and Priestley (1992) stated that "where the wall height is less than three storeys, a greater slenderness should be acceptable. In such cases, or where inelastic flexural deformations cannot develop, the wall thickness t need not be less than $0.05L_n$" (where L_n denotes clear wall length between the supports).

FEMA 306 (1999) also discusses the issue of wall instability. This document also refers to the procedure by Paulay and Priestley (1993) and provides the following recommendation for minimum wall thickness in ductile walls (μ_Δ of 4.0):

$t \le l_w/24$ or $t \le h/18$

Note that the above requirement, which applies to the walls with displacement ductility ratio (μ_Δ) equal to 4.0, is the same as the CSA S304.1-04 requirement for limited ductility walls with R_d equal to 1.5.

FEMA 306 (1999) also points out that "the lack of evidence for this type of failure in existing structures may be due to the large number of cycles at high ductility that must be achieved – most conventionally designed masonry walls are likely to experience other behaviour modes such as diagonal shear before instability becomes a problem."

B.5 Grouting

Limited experimental research evidence indicates that fully grouted reinforced masonry walls demonstrate higher ductility and strength under cyclic lateral loads than otherwise similar partially grouted specimens. Ingham et al. (2001) reported the results of an experimental study of twelve full-scale reinforced masonry wall specimens subjected to an in-plane cyclic lateral

load. Of the twelve specimens, nine were partially grouted, and three were fully grouted. The walls were reinforced with 12 mm diameter vertical reinforcing bars spaced at 800 mm on centre (25% grouted cores), with a bond beam at the top of the wall. The wall thickness varied from 90 mm to 190 mm, which resulted in height/length aspect ratios ranging from 0.57 to 1.33. The walls were not subjected to any external axial load. The walls were designed to fail in the diagonal shear mode. The test results showed that the fully grouted wall specimens demonstrated significantly higher displacement ductility (on the order of 6.0) than the otherwise identical partially grouted specimens (4.0). It should be noted that all of the partially grouted specimens achieved a displacement ductility of 2.0 or higher. A possible reason for the higher ductility in the fully grouted wall specimens is that they ultimately failed in the sliding shear mode, which is characterized by large deformations at the base of the wall. The partially grouted specimens failed in the shear/diagonal tension mode. Force-displacement responses for a partially grouted Wall 2 and a fully grouted Wall 3 specimen are shown in Figure B-6. Note that the specimen dimensions were identical: 2600 mm length x 2400 mm height x 100 mm nominal thickness.

It is important to note that none of the twelve specimens exhibited a sudden failure, as is typically associated with conventional (diagonal tension) shear failure; instead, gradual strength degradation was observed. The findings of related experimental studies by Voon and Ingham (2006) and Schultz (1996) were reported in Section B.1.

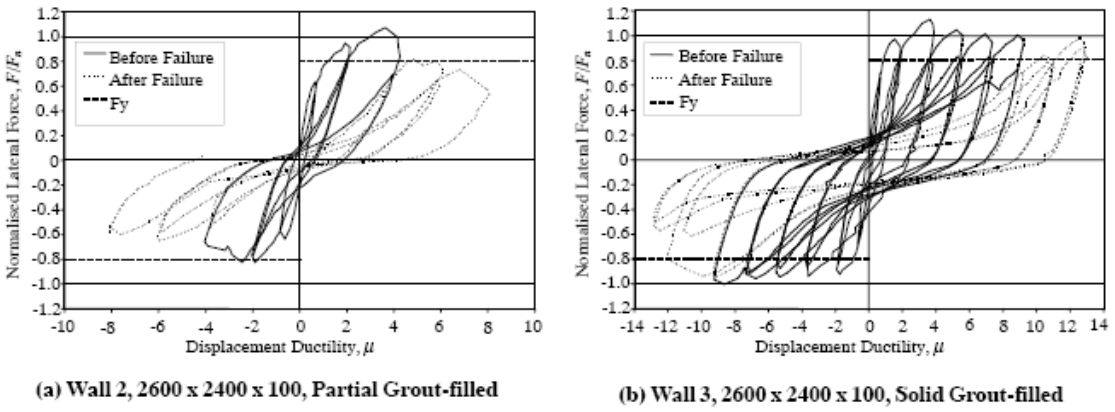

Figure B-6. Force-displacement responses for partially grouted (left) and fully grouted (right) wall specimens (Ingham et al., 2001, reproduced by permission of the Masonry Society).

TABLE OF CONTENTS – APPENDIX C

C Relevant Design Background

This appendix contains additional information relevant for masonry design as discussed in Chapter 2, but it is not directly related to the seismic design provisions of CSA S304.1-04. Applications of design methods and procedures presented in this appendix can be found in Chapter 4, which contains several design examples. The appendix addresses in detail a few topics of interest to masonry designers, e.g., the calculation of in-plane wall stiffness including the effect of cracking, and force distribution in perforated shear walls. However, modeling and analysis of multi-storey perforated shear walls have not been covered in this document.

C.1 Design for Combined Axial Load and Flexure

C.1.1 Reinforced Masonry Walls Under In-Plane Seismic Loading

10.2

Seismic shear forces acting at floor and roof levels cause overturning bending moments in a shear wall, which reach a maximum at the base level. In general, shear walls are subjected to the combined effects of flexure and axial gravity loads. The theory behind the design of masonry wall sections subjected to effects of flexure and axial load is well established, and is essentially the same as that of reinforced concrete walls. A typical reinforced masonry wall section is shown in Figure C-1a, along with the distribution of internal forces and strains arising from the axial load and moment. According to CSA S304.1-04, the strain distribution along the wall length is based on the assumptions that the wall section remains plane and that the maximum compressive masonry strain ε_m is equal to 0.003 (see Figure C-1b). Figure C-1c shows the distribution of internal forces on the base of the wall, as well as the axial load, P_f and the bending moment, M_f. In the compression zone, the equivalent rectangular stress block has a depth a, and a maximum stress intensity of $0.85\chi\phi_m f'_m$. Note that the χ factor assumes the value of 1.0 for members subjected to the compression perpendicular to the bed joints, such as structural walls (S304.1 Cl.10.2.6). Each reinforcing bar develops an internal force (either tension or compression), equal to the product of the factored stress and the corresponding bar area. The internal vertical forces must be in equilibrium with P_f, and the factored moment capacity M_r can be determined by taking the sum of moments of the internal forces around the centroid of the section.

The following three design scenarios and the related simplified design procedures will be discussed in this section:

1. Wall reinforcement (both concentrated and distributed) and axial load are given – find moment capacity
2. Wall is reinforced with distributed reinforcement only – find moment capacity
3. Wall reinforcement needs to be estimated (factored bending moment and axial force are given)

The first two are applicable for the common situations where a designer assumes the minimum seismic reinforcement amount and desires to find its moment capacity.

Approximate design approaches that can be used to assist designers in each of these scenarios are presented below. For detailed analysis and design procedures, the reader is referred to Drysdale and Hamid (2005) and Hatzinikolas and Korany (2005).

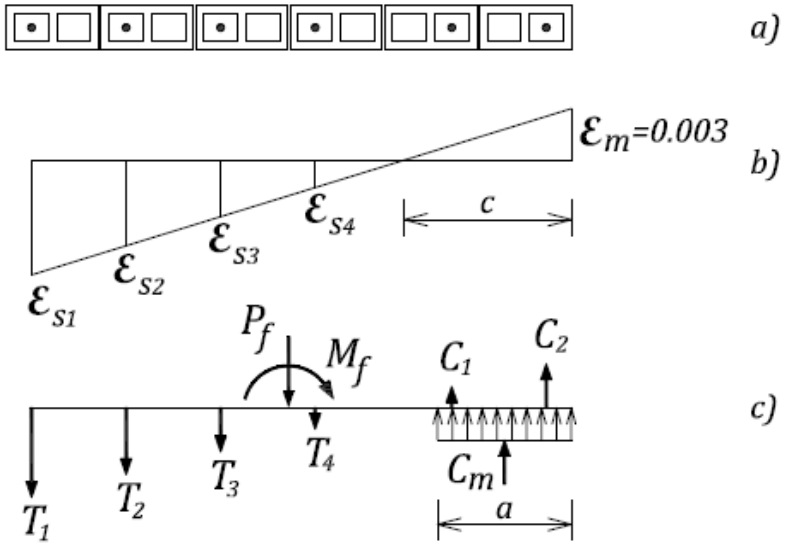

Figure C-1. A reinforced masonry shear wall under the combined effects of axial load and flexure: a) plan view cross section; b) strain distribution; c) internal force distribution.

C.1.1.1 Moment capacity for the section with concentrated and distributed reinforcement

Rectangular section

A simplified wall design model is shown in Figure C-2. The wall reinforcement can be divided into:

- Concentrated reinforcement at the ends (area A_c at each end), and
- Distributed reinforcement along the wall length (total area A_d).

It is assumed that the concentrated wall reinforcement yields either in tension or in compression at the wall ends. Also, it is assumed that the distributed reinforcement yields in tension.

A procedure to find the factored moment capacity M_r for a shear wall with a given vertical reinforcement (size and spacing) is outlined below.

From the equilibrium of vertical forces (see Figure C-2b), it follows that

$$P_f + T_1 + T_2 - C_3 - C_m = 0 \qquad (1)$$

where

$$T_1 = C_3 = \phi_s f_y A_c$$

$$T_2 = \phi_s f_y A_d$$

$$C_m = (0.85\phi_m f'_m)(t \cdot a)$$

The compression zone depth, a, can be determined from equation 1 as follows

$$a = \frac{P_f + \phi_s f_y A_d}{0.85\phi_m f'_m t} \qquad (2)$$

$\beta_1 = 0.8$ when $f'_m < 20$ MPa (note that β_1 value decreases when $f'_m > 20$ MPa, as prescribed in S304.1 Cl.10.2.6)

The neutral axis depth, c, measured from the extreme compression fibre to the point of zero strain is given by

$$c = a/\beta_1$$

Next, the factored moment capacity, M_r, can be determined by summing up the moments around the centroid of the wall section (point **O**) as follows

$$M_r = C_m(l_w - a)/2 + 2\left[\phi_s f_y A_c\left(l_w/2 - d'\right)\right] \qquad (3)$$

where d' is the distance from the extreme compression fibre to the centroid of the concentrated compression reinforcement.

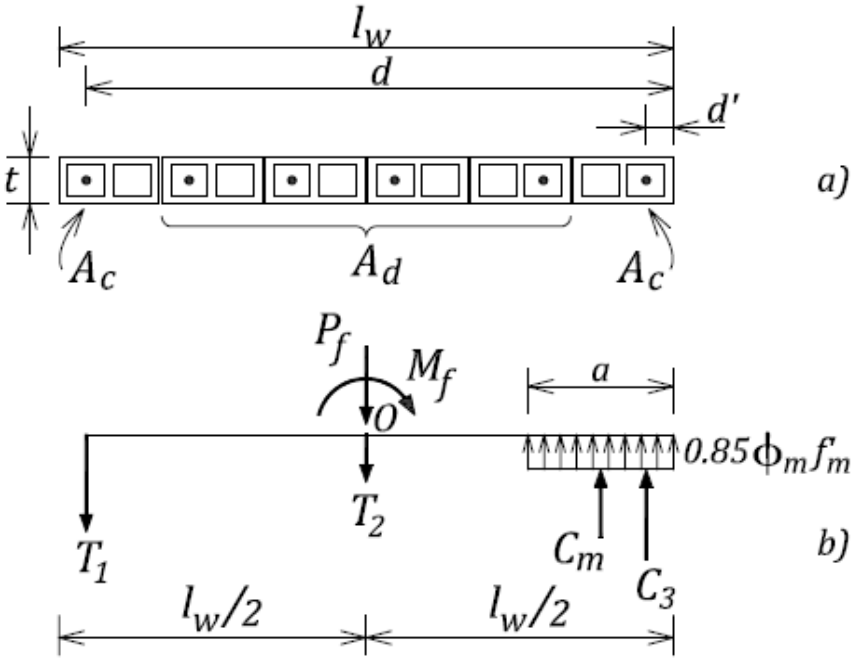

Figure C-2. A simplified design model for rectangular wall section: a) plan view cross-section showing reinforcement; b) internal force distribution.

10.2.8

In case of squat shear walls, CSA S304.1-04 prescribes the use of a reduced effective depth d for flexural design, i.e.

$$d = 0.67 l_w \leq 0.7h$$

As a result, the moment capacity should be reduced by taking a smaller lever arm for the tensile steel, as follows

$$M_r = C_m(l_w - a)/2 + \left[\phi_s f_y A_c\left(l_w/2 - d'\right)\right] + \left[\phi_s f_y A_c\left(d - l_w/2\right)\right] \qquad (4)$$

Note that the reinforcement area A_c in squat walls should be increased to provide more than one reinforcing bar, since the end zone constitutes a larger portion of the overall wall length in these cases.

The CSA S304.1-04 provision for the reduced effective depth in squat walls contained in Cl.10.2.8 is intended to account for the effect of the deep beam behaviour of squat walls. This provision makes more sense for non-seismic design, and it should not be used if the tension steel yields in seismic conditions.

Flanged section

In case of the flanged wall section shown in Figure C- 3, the factored moment capacity M_r can be determined by summing up the moments around the centroid of the wall section (point **O**) as follows

$$M_r = C_m\left(l_w/2 - x\right) + 2\left(\phi_s f_y A_c\right)\left(l_w/2 - d'\right)$$

where

$$a = \frac{A_L - b_f * t + t^2}{t}$$

$$x = \frac{t*\left(a^2/2\right) + (b_f - t)\left(t^2/2\right)}{A_L}$$

A_L is the area of the compression zone.

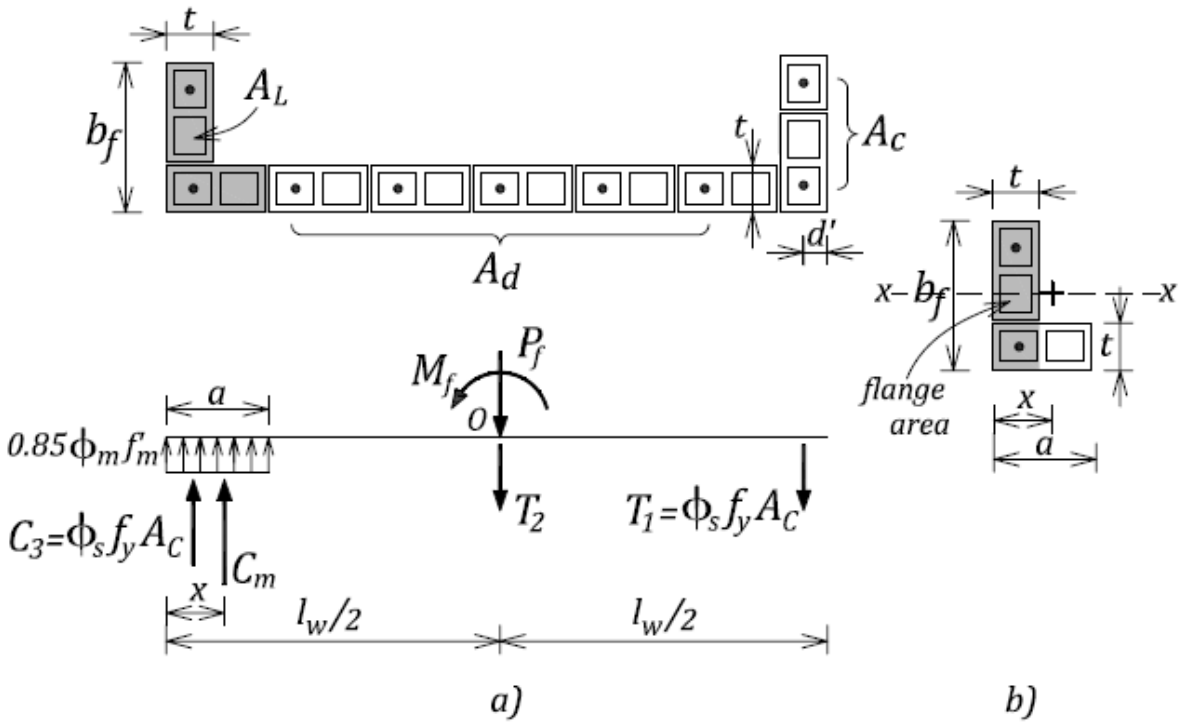

Figure C- 3. A simplified design model for flanged wall section.

C.1.1.2 Moment capacity for rectangular wall sections with distributed vertical reinforcement

The previous section discussed a general case of a shear wall with both concentrated and distributed vertical reinforcement. In low- to medium-rise concrete and masonry wall structures, the provision of distributed vertical reinforcement is often sufficient to resist the effects of combined flexure and axial loads (see Figure C-4a). The factored moment capacity for walls with distributed vertical reinforcement can be determined based on the approximate equation proposed by Cardenas and Magura (1973), which was originally developed for reinforced concrete shear walls. The equation was derived based on the assumption that the distributed wall reinforcement shown in Figure C-4b can be modeled like a thin plate of length l_w (equal to the wall length), and the thickness is such that the total area A_{vt} is the same as that provided by distributed reinforcement along the wall length (see Figure C-4b). The factored moment capacity can be determined as follows:

$$M_r = 0.5\phi_s f_y A_{vt} l_w \left(1 + \frac{P_f}{\phi_s f_y A_{vt}}\right)\left(1 - \frac{c}{l_w}\right) \qquad (5)$$

where

A_{vt} - the total area of distributed vertical reinforcement

c - neutral axis depth

$$\omega = \frac{\phi_s f_y A_{vt}}{\phi_m f'_m l_w t}$$

$$\alpha = \frac{P_f}{\phi_m f'_m l_w t}$$

$$\frac{c}{l_w} = \frac{\omega + \alpha}{2\omega + \alpha_1 \beta_1}$$

$\alpha_1 = 0.85$ and $\beta_1 = 0.8$

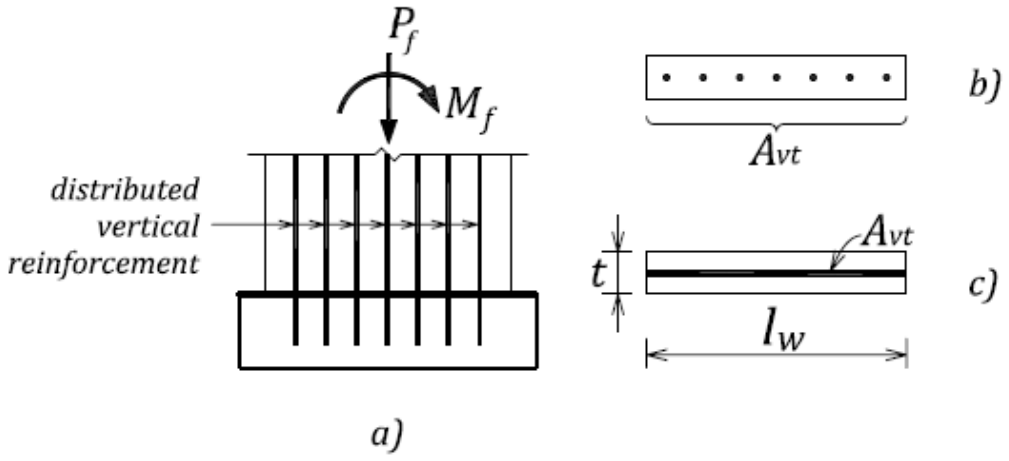

Figure C-4. Shear wall with distributed vertical reinforcement: a) vertical elevation; b) actual cross section; c) equivalent cross-section.

C.1.1.3 An approximate method to estimate the wall reinforcement

Consider a wall cross-section shown in Figure C-5a. In design practice, there is often a need to produce a quick estimate of wall reinforcement based on the given factored loads. In this case, the loads consist of the factored bending moment M_f and axial force P_f acting at the centroid of the wall section (point **O**).

The goal of this procedure is to find the total area of wall reinforcement A_s. To simplify the calculations, an assumption is made that the reinforcement yields in tension and that the resultant force T_r acts at the centroid of the wall section, that is, (see Figure C-5b)

$$T_r = \phi_s f_y A_s \qquad (6)$$

An initial estimate for the compression zone depth a can be made as follows

$$a \cong 0.3 l_w$$

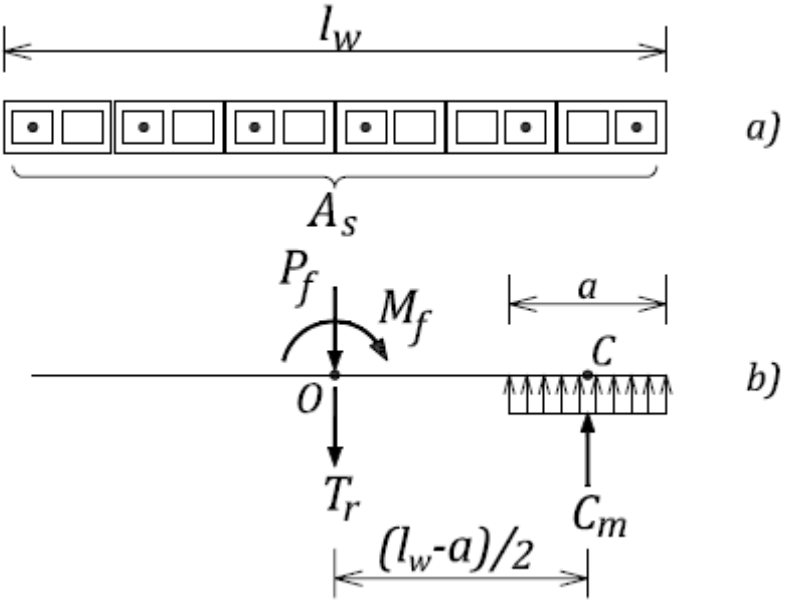

Figure C-5. Reinforcement estimate: a) plan view wall cross-section; b) distribution of internal forces.

Next, compute the sum of moments of all forces around the centroid of the compression zone (point **C**), as follows

$$M_f - P_f (l_w - a)/2 - T_r (l_w - a)/2 = 0$$

From the above equation it follows that

$$T_r = \frac{M_f - P_f (l_w - a)/2}{(l_w - a)/2} \qquad (7)$$

The area of reinforcement can then be determined from equation (7) as follows

$$A_s = T_r / \phi_s f_y$$

The area of reinforcement can be chosen to be equal to or larger than that estimated by this procedure. A uniform reinforcement distribution over the wall length is recommended for seismic design, since research studies have shown that shear walls with uniform reinforcement distribution show better seismic response in the post-cracking range. In addition, the seismic detailing requirements for vertical reinforcement need to be followed.

C.1.2 Reinforced Masonry Walls Under Out-of-Plane Seismic Loading

Masonry walls are subjected to the effects of seismic loads acting perpendicular to their surface – this is called *out-of-plane seismic loading*. For design purposes, wall strips of a predefined width are treated as beams spanning vertically or horizontally between lateral supports. When the walls span in the vertical direction, floor and/or roof diaphragms provide the lateral supports.

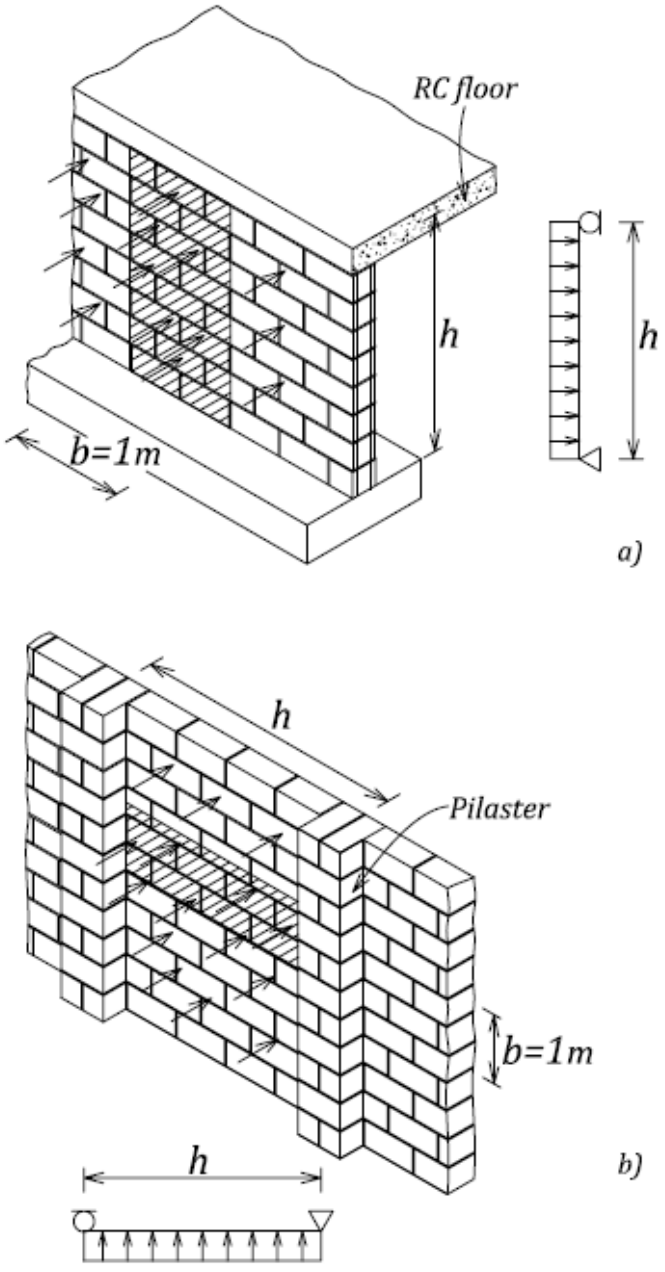

Walls can also span horizontally, in which case the lateral supports need to be provided by cross walls or pilasters, as shown in Figure C-6. Note that support on four edges is very efficient, since these walls behave as two-way slabs.

Figure C-6. Masonry walls under out-of plane seismic loads: a) spanning vertically between floor/roof diaphragms; b) spanning horizontally between pilasters.

Consider a reinforced concrete masonry wall subjected to the effects of factored axial load P_f and bending moment M_f, as shown in Figure C-7a. The wall is reinforced vertically, with only the reinforced cores grouted. It is assumed that the size and distribution of vertical reinforcement are given. The notation used in Figure C-7b is explained below:

t - overall wall thickness (taken as actual block width, e.g. 140 mm, 190 mm, etc.)

t_f - face shell thickness

b - effective width of the compression zone (see Section 2.4.2 and Figure 2-19)

d - effective depth, that is, distance from the extreme compression fibre to the centroid of the wall reinforcement; typically, the reinforcement is placed in the middle of the wall section, so

$d = t/2$

A_s - total area of steel reinforcement placed within the effective width b

It is assumed that the steel has yielded, that is, $\varepsilon_s \geq \varepsilon_y$, and the corresponding stress in the reinforcement is equal to the yield stress, f_y. This is a reasonable assumption for low-rise masonry buildings, since the axial load is low and the walls are expected to fail in the steel-controlled mode. The design procedure is outlined below.

- The resultant forces in steel T_r and masonry C_m can be determined as follows:

  $T_r = \phi_s f_y A_s$

  $C_m = (0.85\phi_m f'_m)(b \cdot a)$

- The equation of equilibrium of internal forces gives (see Figure C-7d)

  $C_m = P_f + T_r$

- The depth of the compression stress block a is equal to

$$a = \frac{C_m}{0.85\phi_m f'_m b} \qquad (8)$$

- The moment resistance can be found from the following equation

$$M'_r = C_m(d - a/2) \qquad (9)$$

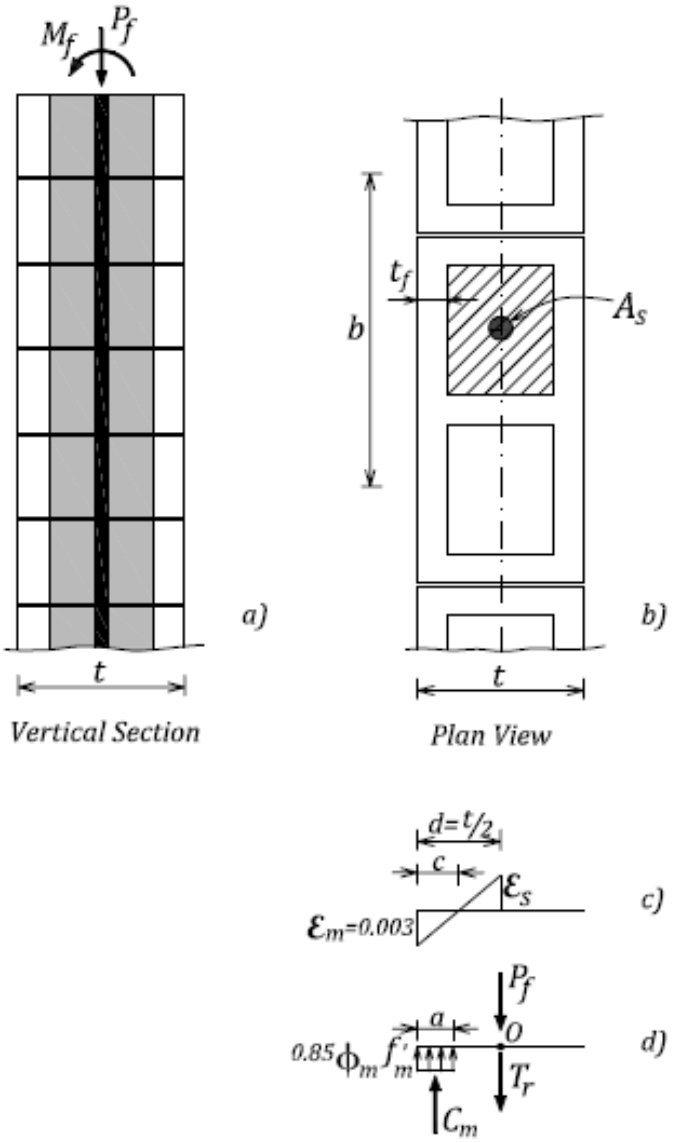

Figure C-7. A wall under axial load and out-of-plane bending: a) vertical section showing factored loads; b) plan view of a wall cross-section; c) strain distribution; d) internal force distribution.

For partially grouted wall sections (where only reinforced cores are grouted), the designer needs to confirm that

$$a \le t_f$$

When the above relation is correct, then the compression zone is rectangular, as shown in Figure C-8a. Note: in solidly grouted walls, the compression zone is always rectangular!

When $a \ge t_f$, the compression zone needs to be treated as a T-section and an additional calculation is required to determine the *a* value. The following equations can be used to determine the moment resistance in sections with a T-shaped compression zone:

- The resultant force in the steel T_r can be determined as follows:

$$T_r = \phi_s f_y A_s$$

- The resultant force in the masonry, C_m, acts at the centroid of the compression zone and can be determined from the equation of equilibrium of internal forces, that is,

$$C_m = P_f + T_r$$

Once the compression force in the masonry is found, the area of the masonry compression zone, A_m (see Figure C-8b), is given by

$$C_m = (0.85\phi_m f'_m) \cdot A_m$$

- The depth of the compression stress block a can be found from the following equation

$$A_m = b \cdot t_f + (a - t_f) \cdot b_w$$

where

b_w = width of the grouted cell plus the adjacent webs

- The distance from the extreme compression fibre to the centroid of the compression zone $\bar{a}$ is equal to

$$\bar{a} = \frac{b \cdot (t_f{}^2/2) + (a - t_f) \cdot \left(t_f + \frac{a - t_f}{2} \right)}{A_m} \qquad (10)$$

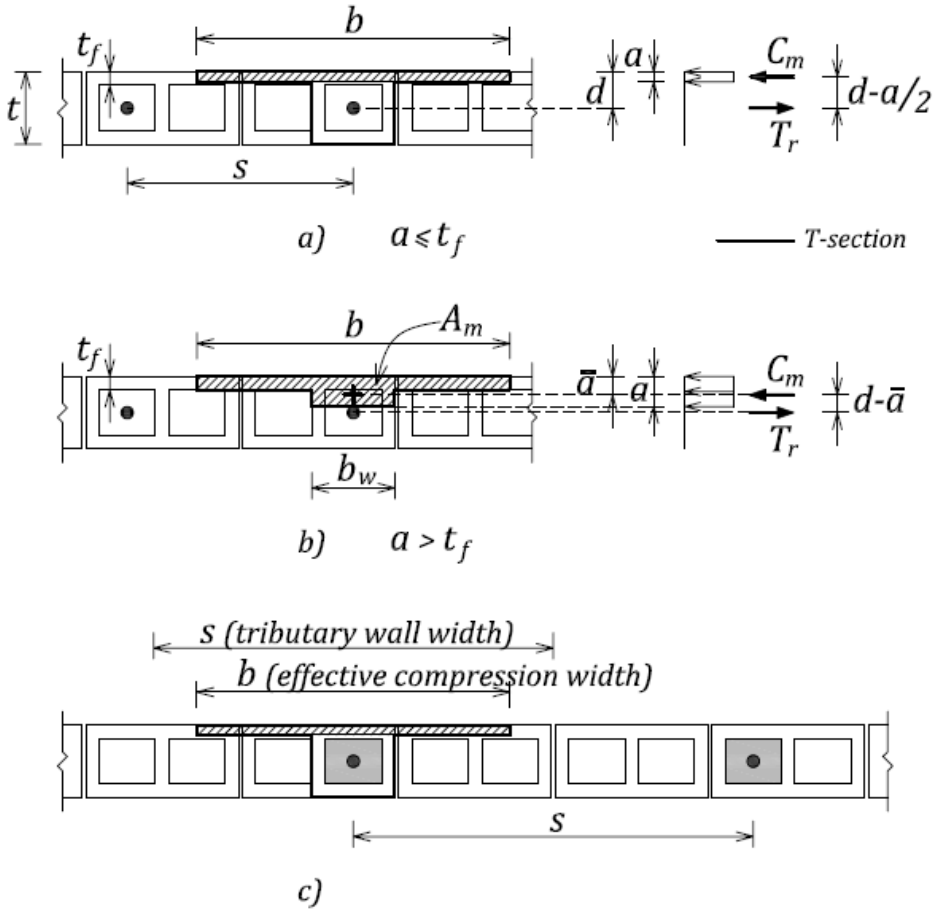

Figure C-8. Masonry compression zone: a) rectangular shape; b) T-shape; c) effective width and tributary width.

- The moment resistance can be found from the following equation

$$M'_r = C_m\left(d - \overline{a}\right) \qquad (11)$$

Note that M'_r denotes the moment capacity for a wall section of width b. It is usually more practical to convert the M'_r value to a unit width equal to 1 metre (see Figure C-8c), as follows

$$M_r = M'_r\left(1.0/s\right) \qquad (12)$$

where

s - spacing of vertical reinforcement expressed in metres (where $b \le s$)

M_r - factored moment capacity in kNm/m.

The design of masonry walls subjected to the combined effects of axial load and bending is often performed using P-M interaction diagrams. The axial load capacity is shown on the vertical axis of the diagram, while the moment capacity is shown on the horizontal axis. The points on the diagram represent the combinations of axial forces and bending moments corresponding to the capacity of a wall cross-section. An interaction diagram is defined by the following four distinct points and/or regions: i) balanced point, ii) points controlled by steel yielding, iii) points controlled by masonry compression, and iv) pure compression (zero eccentricity). A conceptual wall interaction diagram is presented in Figure C-9.

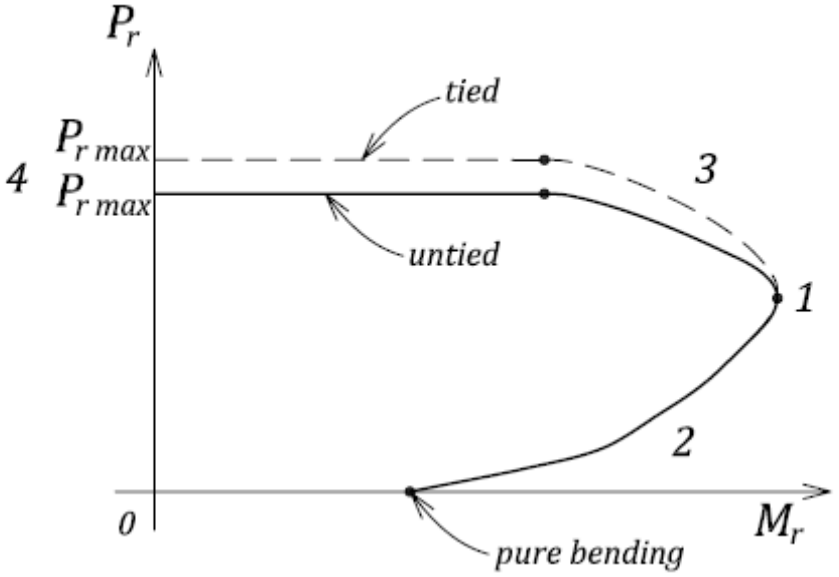

Figure C-9. P-M interaction diagram.

1. Balanced point

At the load corresponding to the balanced point, the steel has just yielded, that is, $\varepsilon_s = \varepsilon_y$. The position of the neutral axis c_b can be determined from the following proportion (see Figure C-7 c):

$$\frac{c_b}{d - c_b} = \frac{\varepsilon_m}{\varepsilon_y}$$

or

$$c_b = d\left(\frac{\varepsilon_m}{\varepsilon_m + \varepsilon_y}\right)$$

For $f_y = 400$ MPa and $\varepsilon_y = 0.002$ it follows that

$c_b = 0.6d$

2. Points controlled by steel yielding

For $c < c_b$, the steel will yield before the masonry reaches its maximum useful strain (0.003). Since the steel is yielding, it follows that $\varepsilon_s > \varepsilon_y$. The designer needs to assume the neutral axis depth (c) value so that $c < c_b$. The compression zone depth can then be calculated as $a = \beta_1 c = 0.8c$ (this is valid for $f'_m < 20MPa$ according to S304.1 Cl.10.2.6). Combinations of axial force and moment values corresponding to an assumed neutral axis depth can be found from the following equations of equilibrium (see Figure C-7d)

$P_r = C_m - T_r$

where

$T_r = \phi_s f_y A_s$ (note that the stress in the steel is equal to f_y since the steel is yielding)

Moment resistance depends on the shape of the masonry compression zone, that is, on whether the section is partially or solidly grouted.

- For a solidly grouted section or a partially grouted section with the compression zone in the face shells only:

$M'_r = C_m(d - a/2)$

where

$C_m = (0.85\phi_m f'_m)(b \cdot a)$

- For a partially grouted section with the compression zone extending into the grouted cells:

$M'_r = C_m(d - \bar{a})$

where

$C_m = (0.85\phi_m f'_m) \cdot A_m$

3. Points controlled by masonry compression

For $c > c_b$, the steel will remain elastic, that is, $\varepsilon_s < \varepsilon_y$ and $f_s < f_y$, while the masonry reaches its maximum strain of 0.003. The designer needs to assume the neutral axis depth (c) value so that $c > c_b$, and the strain in steel can then be determined from the following proportion (see Figure C-7 c):

$$\frac{\varepsilon_m}{d} = \frac{\varepsilon_s}{d - c}$$

thus

$$\varepsilon_s = \varepsilon_m \left(\frac{d - c}{c} \right)$$

The stress in the steel can be determined from Hooke's Law as follows

$f_s = E_s * \varepsilon_s$ (note that steel stress $f_s < f_y$)

where E_s is the modulus of elasticity for steel. The equations of equilibrium are the same as used in part 2 above, except that

$T_r = \phi_s f_s A_s$

The point corresponding to $c = t/2$ is considered as a special case. At that point, the strain distribution is defined by the following values

$\varepsilon_m = 0.003$ and $\varepsilon_s = 0$

thus

$T_r = 0$

4. Pure compression (zero eccentricity)

In the case of pure axial compression (S304.1 Cl.10.4) the axial load resistance for untied sections can be determined as follows:

$P_r = 0.85\phi_m f'_m A_e$ actual axial compression resistance

and

$P_{r\max} = 0.8P_r$ design axial compression resistance

According to S304.1 Cl.10.2.7, when the steel bars are tied by means of joint reinforcement, then the steel contribution can be considered for the compression resistance. The design equation for tied wall sections is as follows:

$P_r = 0.85\phi_m f'_m (A_e - A_s) + \phi_s f_y A_s$

and

$P_{r\max} = 0.8P_r$

C.2 Wall Intersections and Flanged Shear Walls

Flanged shear wall configurations are encountered when a main shear wall intersects a cross-wall (or transverse wall). Examples of flanged walls in masonry buildings are very common, since the bearing wall systems often consist of walls laid in two orthogonal directions. Also, in medium-rise wood frame apartment buildings, elevator shafts are usually of masonry construction, and the intersecting masonry walls that form the core can be considered as flanged walls.

10.6.2

In flanged shear walls, a portion of the cross wall is considered to act as the flange, while the main shear wall acts at the web. Depending on the cross-wall configuration, flanged shear walls may be of I, T- or L-section. An I-section is characterized by the two end flanges, similar to that in Figure C-10 (left), a T-section is characterized with one flanged end and other rectangular/ non-flanged end, while a L-section is characterized by one flanged end (similar to that shown in Figure C-10 right), and other rectangular-shaped (non-flanged) end. Design codes prescribe the maximum effective flange width that may be considered in the shear wall design. The CSA S304.1 requirements for overhanging flange widths for these wall sections are summarized in Table C-1 and Figure C-10. For masonry buildings with substantial flanges the height ratio limits will usually govern.

Table C-1. Overhanging Flange Width Restrictions for T- and L- Section Walls per CSA S304.1 Cl.10.6.2

T-sections (b_T)	**L-sections (b_L)**
$b_T \leq$ the smallest of:	$b_L \leq$ the smallest of:
a) b_{actual}	a) b_{actual}
b) $a_w/2$	b) $a_w/2$
c) $6 \cdot t$	c) $6 \cdot t$
d) $h_w/12$	d) $h_w/16$

where
b_{actual} - actual overhang/flange width
a_w - clear distance between the adjacent cross walls
t - actual flange thickness
h_w - wall height

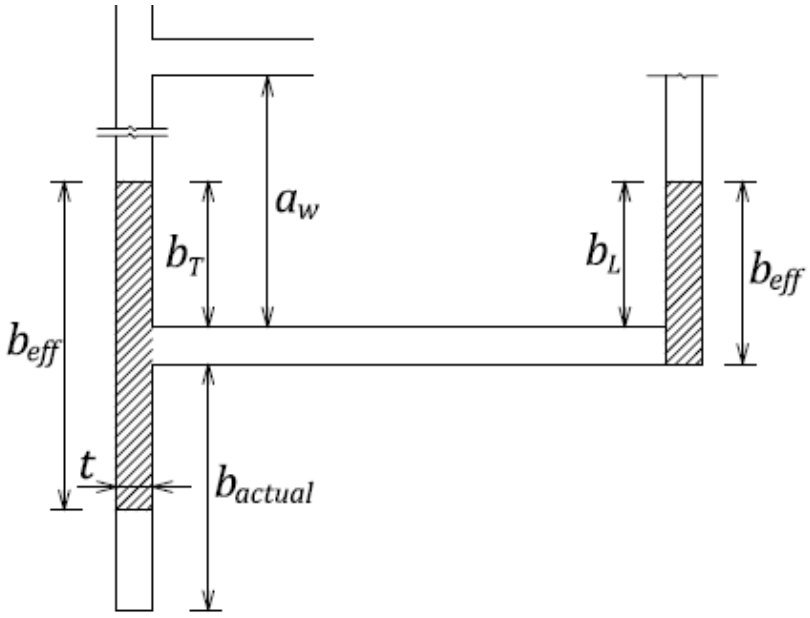

Figure C-10. CSA S304.1 flange width requirements.

7.11 10.11

Flanges do not contribute significantly to the shear resistance of flanged walls, but they generally enhance the in-plane flexural capacity. However, flanges can be considered to be effective in resisting the applied loads only if the web-to-flange joint is capable of transferring the vertical shear. According to CSA S304.1 Cl.7.11, the following alternative approaches can be used to ensure the effective shear transfer across the web-to-flange connection in both unreinforced and reinforced masonry walls (see Figure C-11):

a) Bonded intersections - 50% of the units of one wall embedded at least 90 mm in the other wall (Cl.7.11.1).
b) Mechanical connection with steel connectors (e.g. anchors, rods, or bolts) at a maximum spacing of 600 mm (Cl.7.11.3), and
c) Fully grouted keyways or recesses, with a minimum of two 3.65 mm diameter steel wires from joint reinforcement spaced at 400 mm vertically (Cl.7.11.2).

d) Fully grouted bond beam intersections with15M reinforcing bars spaced as required; this is not explicitly prescribed by CSA S304.1-04, but it is in line with the approach c) outlined in Cl.7.11.3. The bars should be detailed to develop the full yield stress on each side of the intersection.

Note that Cl.10.11.2 does not permit the use of rigid anchors (approach b) for portions of reinforced masonry shear walls in which the flanges contain tensile steel and are subject to axial tension, but alternative solutions are permitted.

Vertical shear resistance of the flanged walls must be checked by one of the following methods:

- For bonded intersections achieved by approach a), vertical shear at the intersection shall not exceed the out-of-plane masonry shear resistance (Cl.7.10.2).
- For flanged sections with the mechanical steel connectors (approach b), the connectors must be capable of resisting the vertical shear at the intersection. The connector resistance should be determined according to CSA A370-04.
- For flanged sections with the horizontal reinforcement (approaches c and d), the reinforcement must be capable of resisting the vertical shear at the intersection.

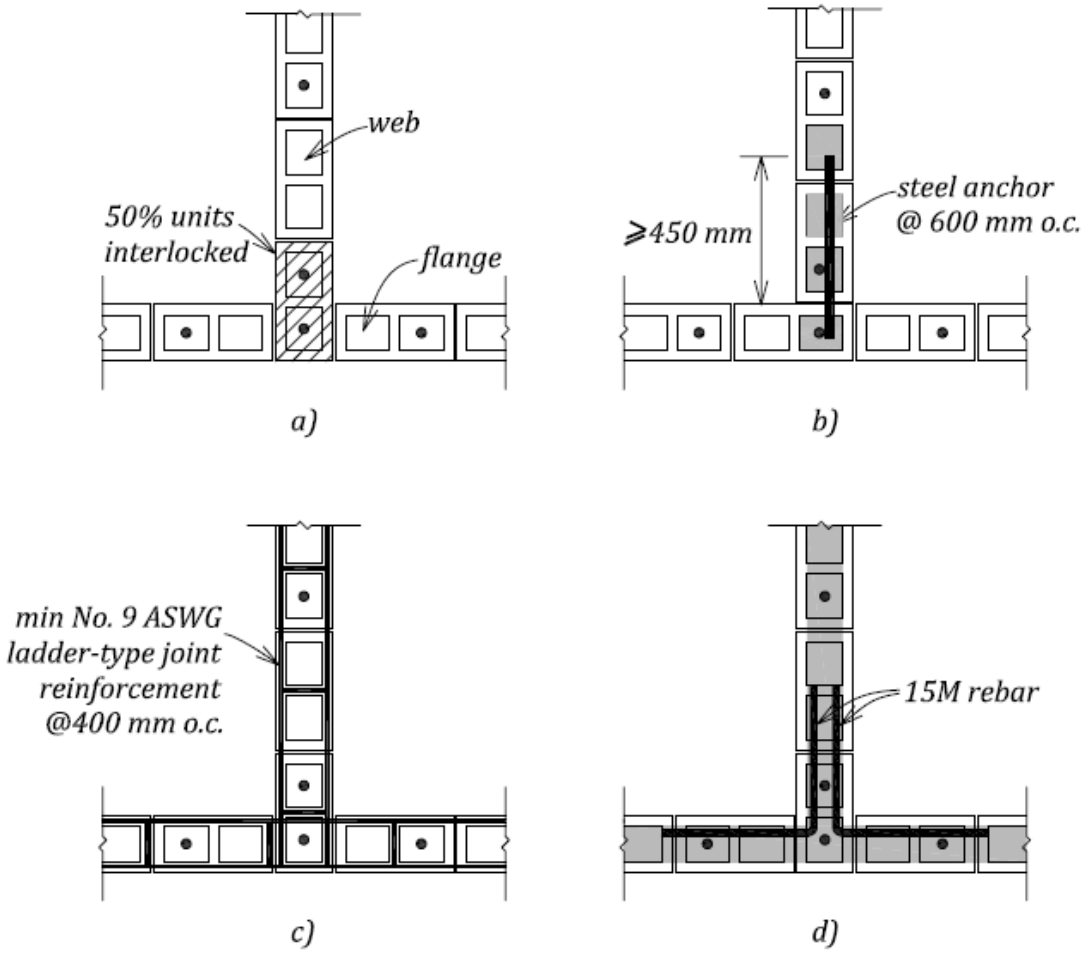

Figure C-11. Masonry wall intersections: a) bonded intersections; b) mechanical connection; c) horizontal joint reinforcement; d) horizontal reinforcing bars (bond beam reinforcement).

7.11.4

Where wall intersections are not bonded and rigid steel connectors are not used, the factored shear resistance of the web-to-flange joint shall be based on the shear friction resistance taken as

$$V_r = \phi_m \mu C_h$$

where

μ = 1.0 coefficient of friction for the web-to-flange joint

C_h = compressive force in the masonry acting normal to the head joint, normally taken as the factored tensile force at yield of the horizontal reinforcement that crosses the vertical section. The reinforcement must be detailed to enable it to develop its yield strength on both sides of the vertical masonry joint, which may be hard to achieve in practice.

Commentary

The provisions related to flanged shear walls have not changed in CSA S304.1-04 from the 1994 edition, with the exception of the new Cl.7.11.4 related to the shear friction resistance of wall intersections.

For flanged walls with horizontal reinforcement, resistance to vertical shear sliding is provided by the frictional forces between the sliding surfaces, that is, the web and the flange of the wall. The shear friction resistance V_r is proportional to the coefficient of friction μ, and the clamping force C_h acting perpendicular to the joint of height h (see Figure C-12a).

C_h is equal to the sum of the tensile yield forces developed in reinforcement of area A_b spaced at the distance s, that is,

$$C_h = \phi_s f_y A_b \, h/s$$

In case of a flanged shear wall with openings, shear friction resistance V_r is provided by wall segments between the openings, as shown in Figure C-12b.

Reinforcement providing the shear friction resistance should be distributed uniformly across the joint. The bars should be long enough so that their yield strength can be developed on both sides of the vertical joint, as shown in Figure C-13b.

Clauses 7.11.1 to 7.11.3 list three approaches (a, b, and c) that can be used to ensure shear transfer at the web-to-flange interface. In addition to the three approaches stated in CSA S304.1-04, it is a common practice in Canada to use 15M reinforcing bars from intersecting bond beams to provide shear resistance if needed (approach d). U.S. masonry design standard ACI 530-08 Cl.1.9.4.2.5 c) prescribes intersecting bond beams in intersecting walls at maximum spacing of 1200 mm (4 ft) on centre. The bond beam reinforcement area shall not be less than 200 mm^2 per metre of wall height (0.1 in^2/ft), and the reinforcement shall be detailed to develop the full yield stress at the intersection.

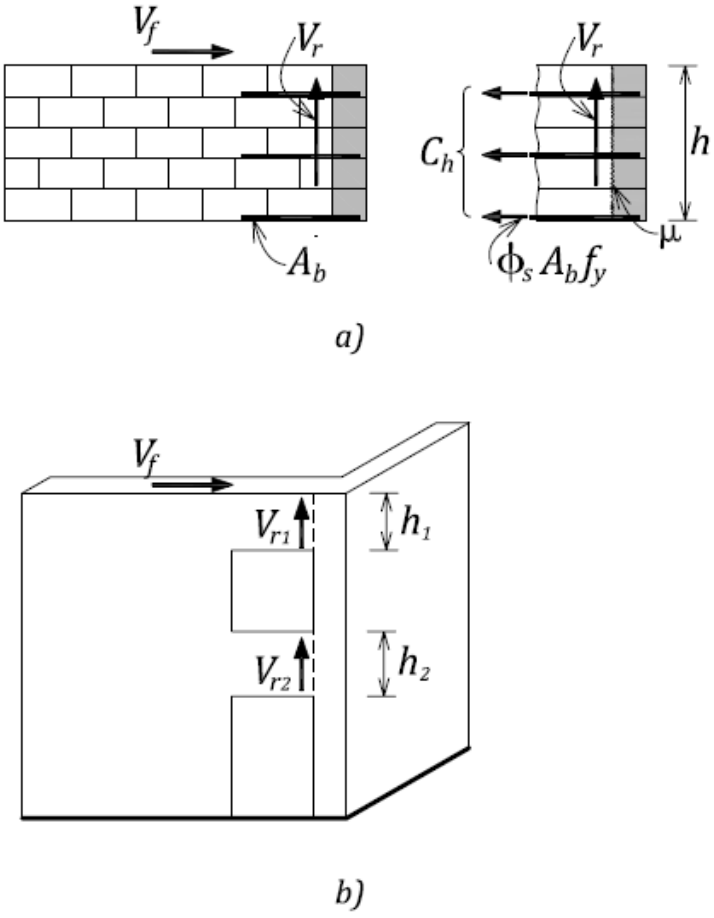

Figure C-12. Shear friction resistance at the web-to-flange intersection: a) resistance provided by the reinforcement; b) flanged shear wall with openings.

When the shear resistance of the web-to-flange interface relies on masonry only (see Figure C-13a), the horizontal shear stress v_f, due to shear force V_f, can be given by:

$$v_f = \frac{V_f}{t_e l_w}$$

where

t_e - effective web width

l_w - wall length

The designer should also find the vertical shear stress caused by the resultant compression force P_{fb}:

$$v_f = \frac{P_{fb}}{b_w * h_w}$$

The larger of these two values governs. The factored shear stress should be less than the factored masonry shear resistance, $\phi_m v_m$, as follows

$$v_f \le \phi_m v_m$$

where

$v_m = 0.16\sqrt{f'_m}$

If the above condition is not satisfied, horizontal reinforcement needs to be provided (see Figure C-13b), and the following shear resistance check should be used

$v_f \le \phi_m v_m + v_s$

where v_s is the factored shear resistance provided by the steel reinforcement, which can be determined as follows:

$$v_s = \frac{\phi_s A_b f_y}{s \cdot t_e}$$

where A_b is area of horizontal steel reinforcement crossing the web-to-flange intersection at the spacing s.

Note that the reinforcement that crosses the vertical section has to be detailed to develop yield strength on both sides of the vertical masonry joint (see Figure C-13b).

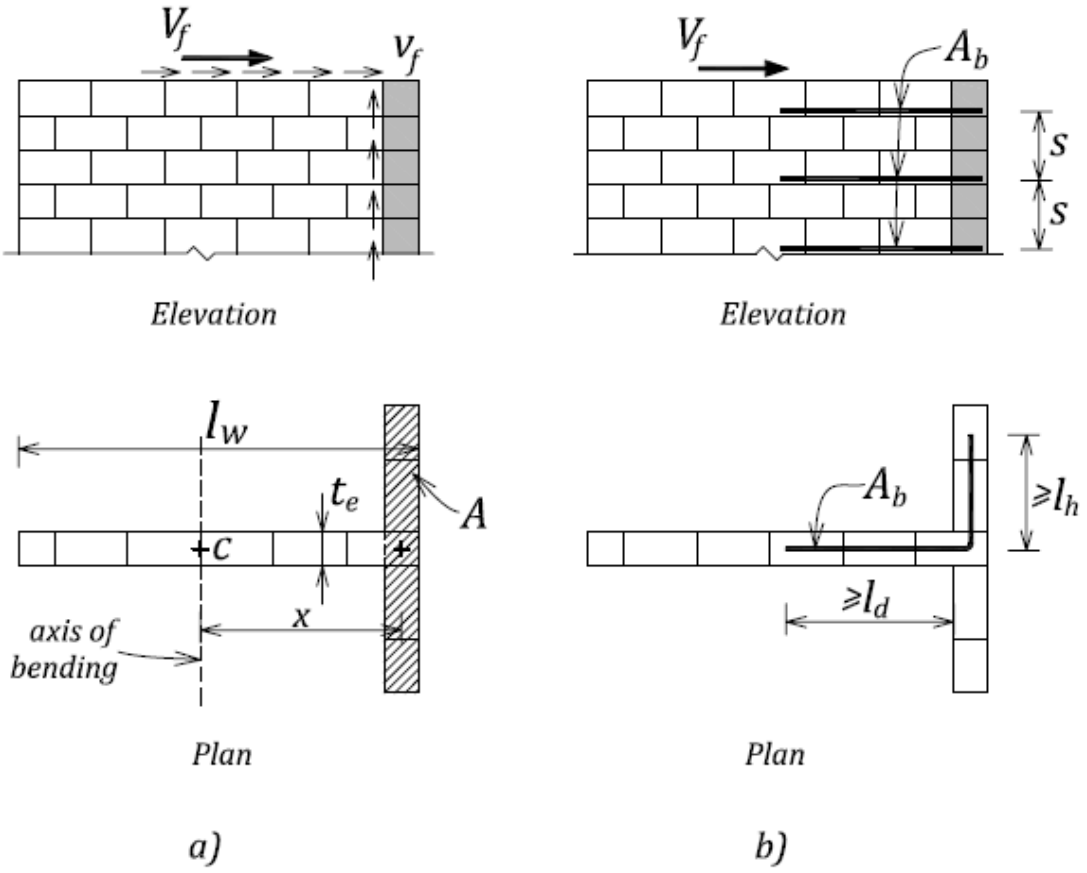

Figure C-13. Shear resistance of the web-to-flange interface: a) bonded masonry intersection; b) horizontal reinforcement at the intersection.

C.3 Wall Stiffness Calculations

The determination of wall stiffness is one of the key topics in the seismic design of masonry walls. Although this topic has been covered in other references (e.g. Drysdale and Hamid, 2006, and Hatzinikolas and Korany, 2006), a few key concepts are discussed in this section. Section C.3.2 derives expressions for the in-plane lateral stiffness of walls under the assumption that the walls are uncracked. For seismic analysis it is expected that the walls will be pushed into the nonlinear range, and so cracking will occur and the reinforcement will yield. The stiffness to be used in seismic analysis should not be the linear elastic (uncracked) stiffness but some effective stiffness that reflects the effect of cracking up to the yield capacity of the wall. Section C.3.5 gives some suggestions for the effective stiffness of shear walls responding in shear-dominant and flexure-dominant modes.

C.3.1 Lateral Load Distribution

The distribution of lateral seismic loads to individual walls can be performed once the storey shear forces have been determined from the seismic analysis. The flexibility of floor and/or roof diaphragms is one of the key factors influencing the load distribution (for more details, see Section 1.5.9 and Example 3 in Chapter 4). In the case of a flexible diaphragm, the lateral storey forces are usually distributed to the individual walls based on the tributary area. In the case of a rigid diaphragm, these forces are distributed in proportion to the stiffness of each wall. In calculating the wall forces, torsional effects must be considered, as discussed in Section 1.5.9. The distribution of lateral loads (without torsional effects) in a single-storey building with a rigid diaphragm is shown in Figure C-14.

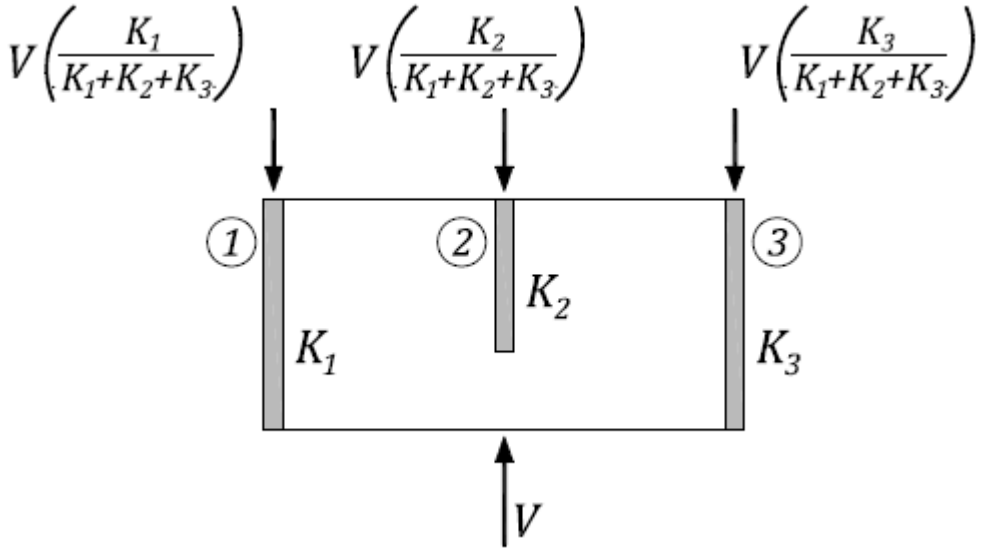

Figure C-14. Distribution of lateral loads to individual walls.

Wall stiffness is usually determined from the elastic analysis, and depends on wall height/length aspect ratio, thickness, mechanical properties, extent of cracking, size and location of openings, etc.

C.3.2 Wall Stiffness: Cantilever and Fixed-End Model

Wall stiffness depends on the end support conditions, that is, whether a wall or pier is fixed or free to move and/or rotate at its ends. Two models for wall stiffness include the cantilever model and the fixed-end model shown in Figure C-15. In the cantilever model, the wall is free to rotate and move at the top in the horizontal direction – this is usually an appropriate model for the walls in a single-storey masonry building.

The stiffness can be defined as the lateral force required to produce a unit displacement, but it is determined by taking the inverse of the combined flexural and shear displacements produced by a unit load. It should be noted that flexural displacements will govern for walls with an aspect ratio of 2 or higher. For example, the contribution of shear deformation in a wall with a height/length aspect ratio of 2.0, is 16% for the cantilever model and 43% for the fixed-end model. The stiffness equations presented in this section take into account both shear and flexural deformations.

The stiffness of a cantilever wall or a pier can be determined from the following equation (see Figure C-15 a):

$$\frac{K}{E_m * t} = \frac{1}{\left(\frac{h}{l_w}\right)\left[4\left(\frac{h}{l_w}\right)^2 + 3\right]} \qquad (13)$$

The stiffness of a wall or a pier with the fixed ends can be determined from the following equation (see Figure C-15 b):

$$\frac{K}{E_m * t} = \frac{1}{\left(\frac{h}{l_w}\right)\left[\left(\frac{h}{l_w}\right)^2 + 3\right]} \qquad (14)$$

where

h - wall height (cantilever model) or clear pier height (fixed-end model)

l_w - wall or pier length

$E_m = 850\, f'_m$ modulus of elasticity for masonry

The following assumptions have been taken in deriving the above equations:

$G_m = 0.4E_m$ modulus of rigidity for masonry (shear modulus)

$I = \frac{t_e * l_w^{\,3}}{12}$ uncracked wall moment of inertia

$A_v = \frac{5 * t_e * l_w}{6}$ shear area (applies to rectangular wall sections only)

where t_e = effective wall thickness.

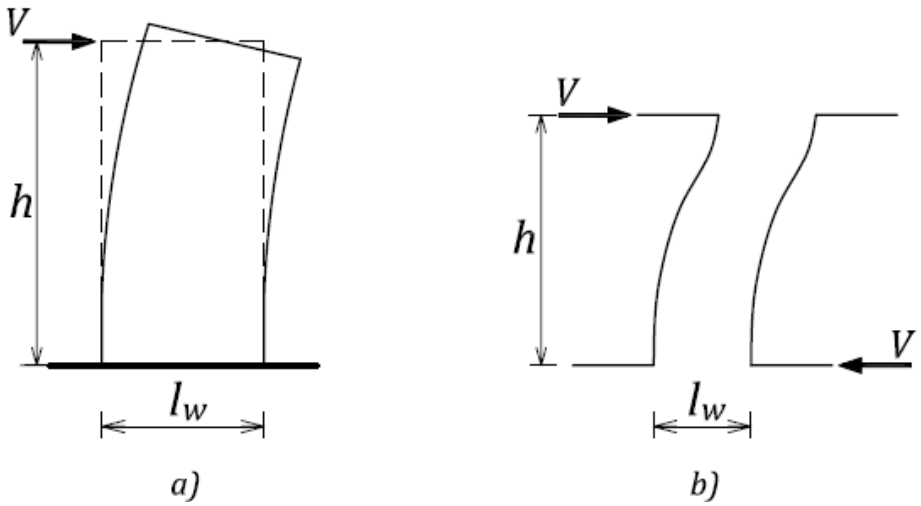

Figure C-15. Wall stiffness models: a) cantilever model, and b) fixed-end model.

The wall stiffnesses for both models for a range of height/length aspect ratios are presented in Table D-3. Note that the derivation of stiffness equations has been omitted since it can be found in other references (see Hatzinikolas and Korany, 2005).

C.3.3 Approximate Method for Force Distribution in Masonry Shear Walls

In most real-life design applications, walls are perforated with openings (doors and windows). The seismic shear force in a perforated wall can be distributed to the piers in proportion to their stiffnesses. This approach is feasible when the openings are very large and the stiffness of lintel beams is small relative to the pier stiffnesses, or if the lintel beam is very stiff so that connected piers act as fixed-ended walls. Figure C-16 illustrates the distribution of wall shear force V to individual piers in direct proportion to their stiffness. Note that, according to this model, the wall shear force is equal to the sum of shear forces in the piers, that is,

$$V = \sum V_i$$

where

$V_i = K_i * \Delta_i$ force in the pier i

Thus

$$V = \sum (K_i * \Delta_i)$$

If the floor diaphragm is considered to be rigid, it can be assumed that the lateral displacement in all piers is equal to Δ, that is,

$$\Delta_A = \Delta_B = \Delta_C = \Delta$$

and so

$$V = (\sum K_i) * \Delta$$

Thus

$$\Delta = \frac{V}{\sum K_i}$$

where

$$K = \sum K_i$$

denotes the overall wall stiffness for the system.

Therefore, the force in each pier is proportional to its stiffness relative to the sum of all pier stiffnesses within the wall, as follows

$$V_i = K_i * \Delta_i = K_i * \frac{V}{\sum K_i} = V * \frac{K_i}{\sum K_i}$$

This means that stiffer piers are going to attract a larger portion of the overall shear force. This can be explained by the fact that a larger fraction of the total lateral force is required to produce the same deflection in a stiffer wall as in a more flexible one.

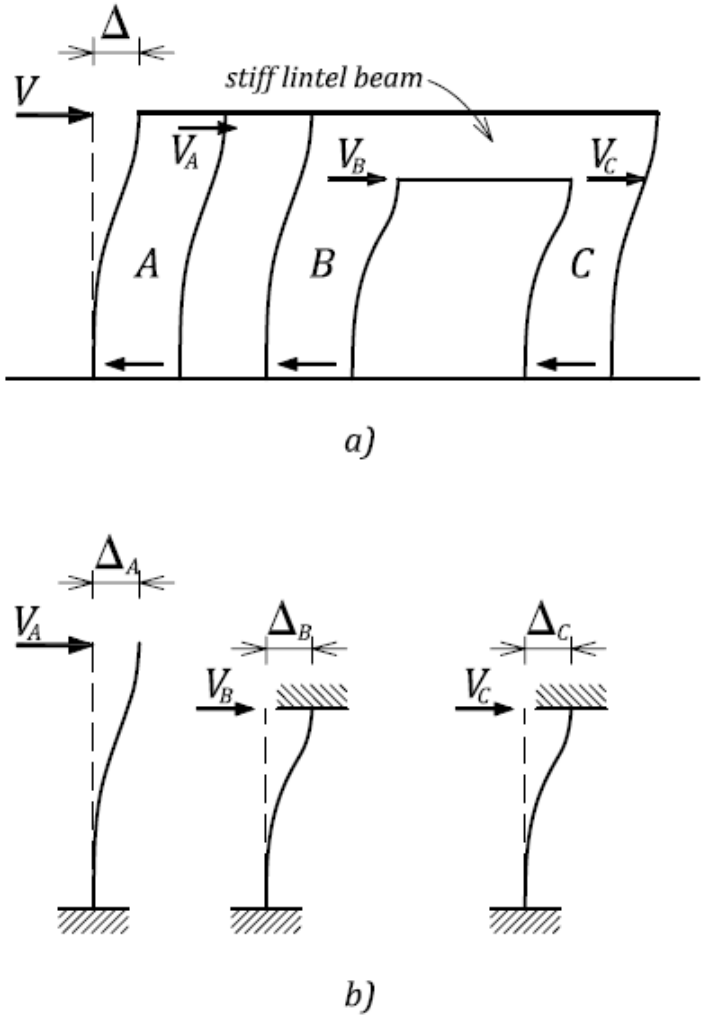

Figure C-16. Shear force distribution in a wall with a rigid diaphragm: a) wall in the deformed shape: b) pier forces.

An approximate approach for determining the stiffness of a solid shear wall in a multi-storey building is to consider the structure as an equivalent single-storey structure, as shown in Figure C-17. The entire shear force is applied at the effective height, h_e, defined as the height at which the shear force V_f must be applied to produce the base moment M_f, that is,

$$h_e = \frac{M_f}{V_f}$$

The wall stiffness is found to be equal to the reciprocal of the deflection at the effective height Δ_e, as follows

$$K = \frac{1}{\Delta_e}$$

This model, although not strictly correct, can be used to determine the elastic distribution of the torsional forces as well as the displacements, as illustrated in Example 2 in Chapter 4.

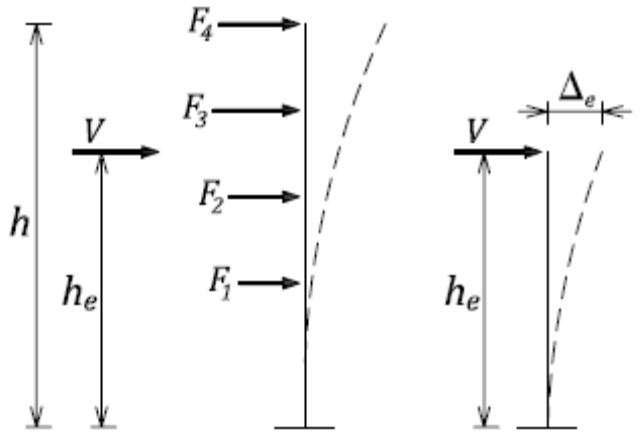

Figure C-17. Vertical combination of wall segments with different stiffness properties.

Several different elastic analysis approaches can be used to determine the stiffness of a wall with openings. A simplified approach suitable for the stiffness calculation of a perforated wall in a single-storey building can be explained with the help of an example of the wall X_1 shown in Figure C-18 (see also Example 3 in Chapter 4). For a unit load applied at the top, the wall stiffness calculation involves the following steps:

- First, calculate the deflection at the top for a cantilever wall, considering the wall to be solid (Δ_{solid}).
- Next, calculate the deflection for the strip containing openings (Δ_{strip}), considering the full wall length (i.e. ignore openings).
- Finally, calculate the deflection for the piers A, B, C, and D (Δ_{ABCD}) assuming that all piers have the same deflection.

Note that the deflections for individual components are calculated as the inverse of their stiffness values, and that the pier stiffnesses are determined assuming either the cantilever or fixed-end models. In most cases, the use of the cantilever model is more appropriate.

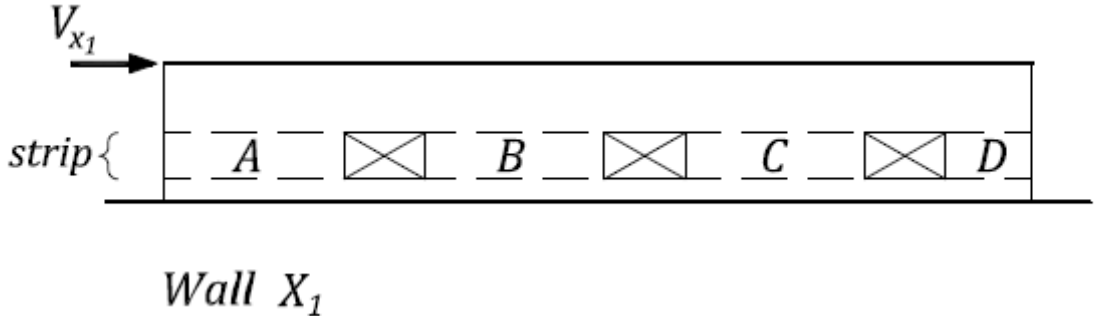

Figure C-18. An example of a perforated wall.

The overall wall deflection can be determined by combining the deflections for these components, as follows:

$$\Delta = \Delta_{solid} - \Delta_{strip} + \Delta_{ABCD}$$

Note that the strip deflection is subtracted from the solid wall deflections - this removes the entire portion of the wall containing all the openings, which is then replaced by the four segments.

Finally, the wall stiffness is equal to the reciprocal of the deflection, as follows

$$K = \frac{1}{\Delta}$$

C.3.4 Advanced Design Approaches for Reinforced Masonry Shear Walls with Openings

The approximate approach based on elastic analysis presented in Section C.3.3 is appropriate for determining the lateral force distribution in masonry walls. However, that method is not adequate for predicting the strengths in perforated reinforced masonry shear walls (walls with openings). Openings in a masonry shear wall alter its behaviour and add complexity to its analysis and design. When the openings are relatively small, their effect can be ignored, however in most walls the openings need to be considered. The following two design approaches can be used to design walls with openings:

1) Plastic analysis method, and
2) Strut-and-tie method.

These two approaches have been evaluated by experimental studies and have shown very good agreement with the experimental results (Voon, 2007; Elshafie et al., 2002; Leiva and Klingner, 1994). The key concepts will be outlined in this section.

C.3.4.1 Plastic analysis method

The plastic analysis method, also known as limit analysis, can be used to determine the ultimate load-resisting capacity for statically indeterminate structures. A masonry wall with an opening as shown in Figure C-19a can be modeled as a frame (see Figure C-19b). The model is subjected to an increasing load until the flexural capacity of a specific section is reached and a *plastic hinge* is formed at that location. (The plastic hinge is a region in the member that is assumed to be able to undergo an infinite amount of deformation, and can therefore be treated as a hinge for further analysis.) With further load increases, plastic hinges will be formed at other sections as their flexural capacity is reached. This process continues until the system becomes statically determinate, at which point the formation of one more plastic hinge will result in a collapse under any additional load. This is called a collapse mechanism, and an example is shown in Figure C-19c. There is usually more than one possible collapse mechanism for a statically indeterminate structure, and the mechanism that gives the lowest capacity is closest to the ultimate capacity, as this is an upper bound method.

For specific application to perforated masonry walls, the wall is idealized as an equivalent frame, where piers are modeled as fixed at the base and either pinned or fixed at the top, while lintels are modeled as fixed at the ends. A failure state is reached when plastic hinges form at member ends, and the collapse mechanism forms. The sequence of plastic hinge formation depends on the relative strength and stiffness of the elements. In this approach, structural members must be designed to behave mainly in a flexural mode, while a shear failure is avoided by applying the capacity design approach.

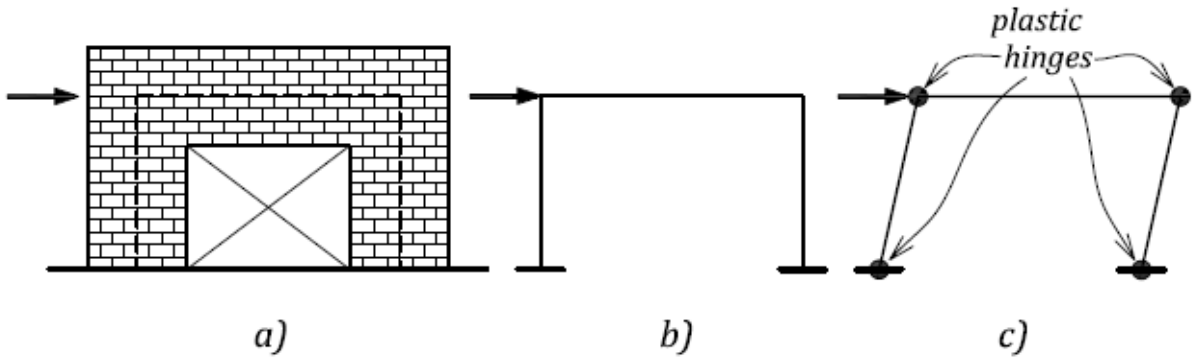

Figure C-19. An example of a plastic collapse mechanism for a frame system: a) perforated masonry wall; b) frame model; c) plastic collapse mechanism.

The following two mechanisms are considered appropriate for the plastic analysis of reinforced masonry walls with openings, as shown in Figure C-20 (Leiva and Klingner, 1994; Leiva et al. 1990):

1) pier mechanism, and

2) coupled wall mechanism.

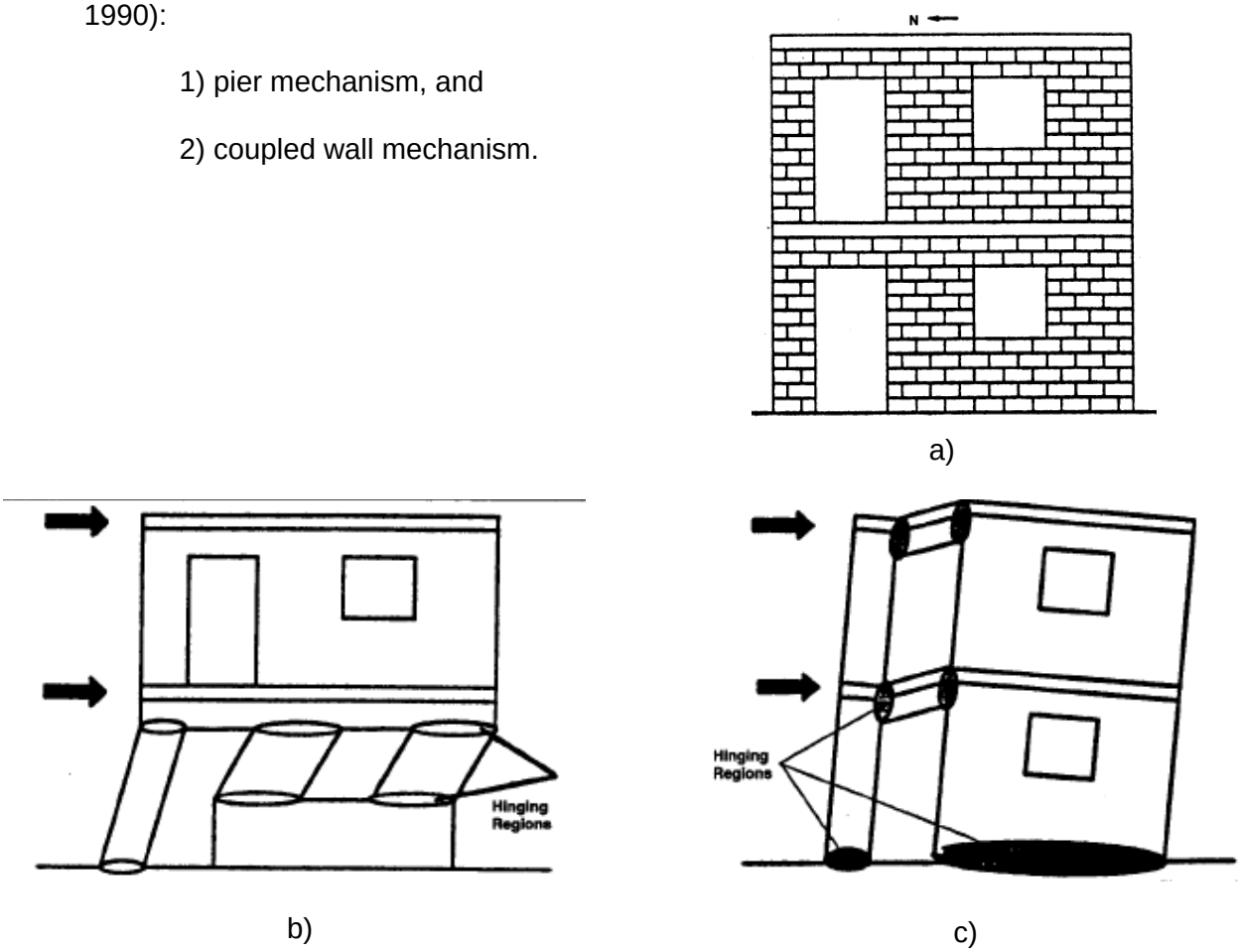

Figure C-20. Plastic analysis models for perforated walls: a) actual wall; b) pier model; c) coupled wall model (Leiva and Klingner, 1994, reproduced by permission of the Masonry Society).

A pier mechanism is a collapse mechanism with flexural hinges at tops and bottoms of the piers. A pier-based design philosophy visualizes a perforated wall as a ductile frame. Horizontal reinforcement above and below the openings is needed to transfer the pier shears into the rest of the wall. A drawback of the pier mechanism is that the formation of plastic hinges at the top and bottom of all piers at a story level can lead to significant damage to the piers, which are the main vertical load-carrying elements.

A coupled wall mechanism is a collapse mechanism in which flexural hinges are formed at the base of the wall and at the ends of the coupling lintels. A perforated wall is modeled as a series of ductile coupled walls; this concept is similar to that used for seismic design of reinforced concrete shear walls. The vertical reinforcement in each pier must be designed so that the flexural capacity of the piers exceeds the flexural capacity of the coupling beams. To achieve this, additional longitudinal reinforcement is placed in the piers, but cut off before it reaches the wall base. The shear reinforcement in the coupling beams is designed based on the flexural and shear capacity of the piers. Since masonry walls are usually long in plan, the formation of plastic hinges at their bases produces large strains in the wall longitudinal reinforcement. Plastic hinges must have adequate rotational capacity to allow the complete mechanism to form; this can be achieved in wall structures with low axial load. To ensure the successful application of the plastic analysis method, the wall reinforcement must be detailed to develop the necessary strength and inelastic deformation capacity.

Figure C-21 shows a simple single-storey wall that is analyzed for the two mechanisms. Ultimate shear forces corresponding to the pier and coupled wall mechanisms can be determined from the equations of equilibrium assuming that the moments at the plastic hinge locations are known. These equations are summarized in Figure C-21 (Elshafaie et al., 2002).

The plastic analysis method has a few advantages: stiffness calculations are not required, and the designer can choose the failure mechanism which ensures a desirable ductile response. The designer needs to have a general background in plastic analysis, which is covered in several references, e.g. Bruneau, Uang, and Whittaker (1998) and Ferguson, Breen, and Jirsa (1988). This method is also used for the seismic analysis of concrete and steel structures, and is referred to as nonlinear static analysis or pushover analysis.

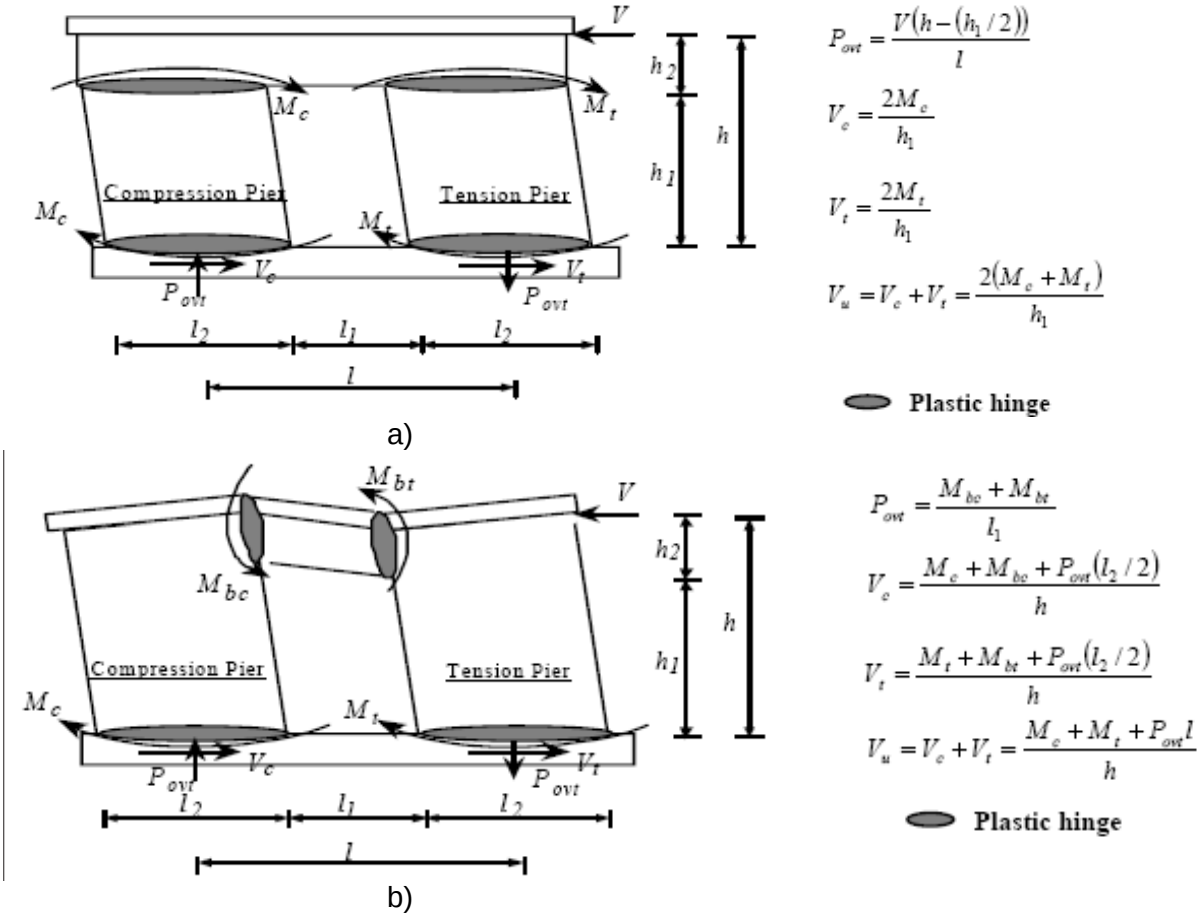

Figure C-21. Ultimate wall forces according to the plastic analysis method: a) pier mechanism; b) coupled wall mechanism (Elshafaie et al., 2002, reproduced by permission of the Masonry Society).

C.3.4.2 Strut-and-Tie Method

The strut-and-tie method essentially follows the truss analogy approach used for shear design of concrete and masonry structures. Pin-connected trusses consist of steel tension members (ties), and masonry compression members (struts). The masonry compression struts develop between parallel inclined cracks in the regions of high shear. The essential feature of this approach is that the designer needs to find a system of internal forces that is in equilibrium with the externally applied loads and support conditions. A further essential feature is that the designer must ensure that the steel and masonry tie members provided adequately resist the forces obtained from the truss analysis.

The design of tension ties is particularly important. If a ductile response is to be assured, the designer should choose particular tension chords in which yielding can best be accommodated. Other ties can be designed so that no yielding will occur by using the capacity design approach. The magnitudes of the forces in critical tension ties can be determined from statics, corresponding to the overturning moment capacity of the wall using the nominal material properties (rather than the factored ones). The remaining forces are then determined from the equilibrium of nodes (conventional truss analysis). Compression forces developed in masonry struts are usually small due to the small compression strains and do not govern the design.

Careful detailing of the wall reinforcement is necessary to ensure that the actual structural response will correspond to that predicted by the analytical model.

The designer needs to use judgement to simplify the force paths that are chosen to represent the real structure – these differ considerably depending on individual judgement.

An example of a strut-and-tie model for a two-storey perforated masonry wall subjected to seismic lateral load is shown in Figure C-22 (note that gravity load also needs to be considered in the analysis, however it is omitted from the figure). It can be seen that two different models are required to account for the alternate direction of seismic load. The examples show the seismic load being applied as a compressive load to the building; however, these loads should be applied to the floor levels, depending on the diaphragm-to-wall connection. The designated tie members in one model will become struts in the other model (when the seismic load changes direction). An advantage of the reversible nature of seismic forces is that a significant fraction of the inelastic tensile strains imposed on the end strut members is recoverable due to force reversal, thereby providing hysteretic energy dissipation. A detailed solution for this example is presented in the User's Guide by NZCMA (2004).

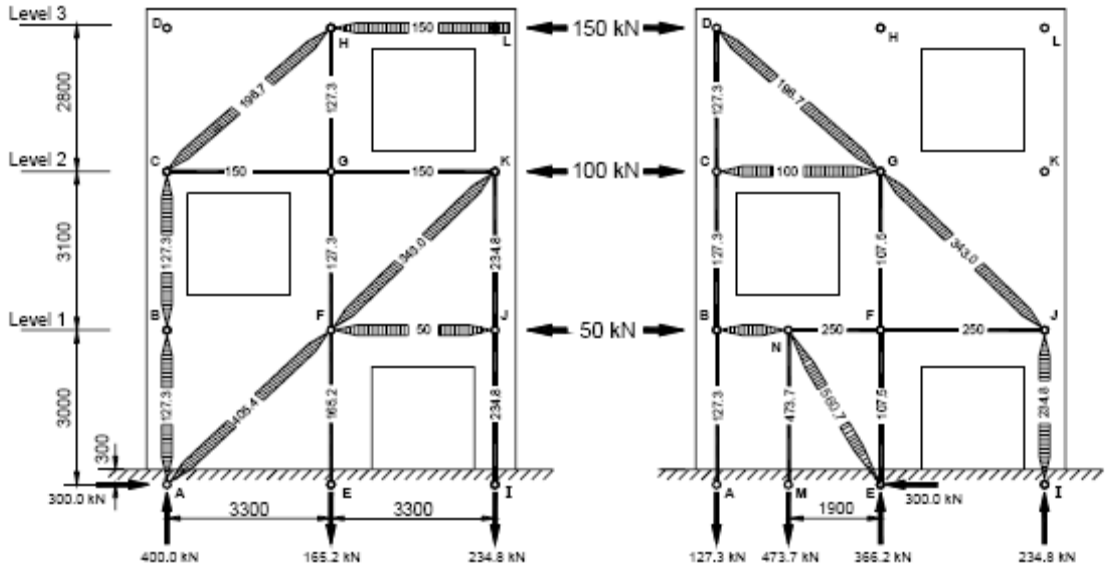

Figure C-22. Strut-and-tie models for a masonry wall corresponding to different directions of seismic loading (NZCMA, 2004, reproduced by the permission of the New Zealand Concrete Masonry Association Inc.).

Strut-and-tie models are used for design of masonry walls in New Zealand, and this approach is explained in more detail by Paulay and Priestley (1992). The New Zealand Masonry Standard NZS 4230:2004 (SANZ, 2004) recommends the use of strut-and-tie models for the design of perforated reinforced masonry shear walls. In Canada, strut-and-tie models are used to design discontinuous regions of reinforced concrete structures according to the Standard CSA A23.3-04 Design of Concrete Structures. The design concepts and applications of strut-and-tie models for concrete structures in Canada are covered by McGregor and Bartlett (2000).

C.3.5 The Effect of Cracking on Wall Stiffness

The behaviour of masonry walls under seismic load conditions is rather complex, and depends on the failure mechanism (shear-dominant or flexure-dominant), as discussed in Section 2.3.1. Figure C-23 shows the hysteretic response of shear-dominant and flexure-dominant walls. The effective stiffness discussed in this section reflects the secant stiffness up to first crack in the brittle shear-dominant walls, and the stiffness for an elastic-perfectly-plastic model that would approximate the strength envelope of the hysteretic plot in the ductile flexure-dominant walls.

For the *shear-dominant mechanism*, the response is initially elastic until cracking takes place, at which point there is a substantial drop in stiffness. This is particularly pronounced after the development of diagonal shear cracks. After a few major cracks develop, the load resistance is taken over by the diagonal strut mechanism, and the shear stiffness can be estimated by an appropriate strut model. However, the stiffness drops significantly shortly after the strut mechanism is formed, and can be considered to be zero for most practical purposes (see Figure C-23a). It is expected that an increase in the quantity of vertical and horizontal steel and/or the magnitude of axial compressive stress causes a reduced crack size and an increase in the shear stiffness (Shing et al., 1990).

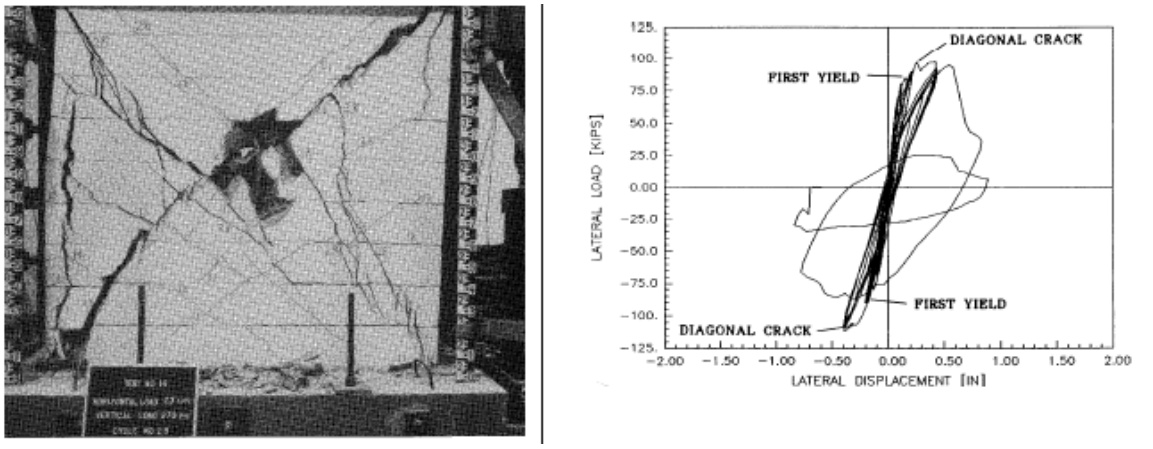

a)

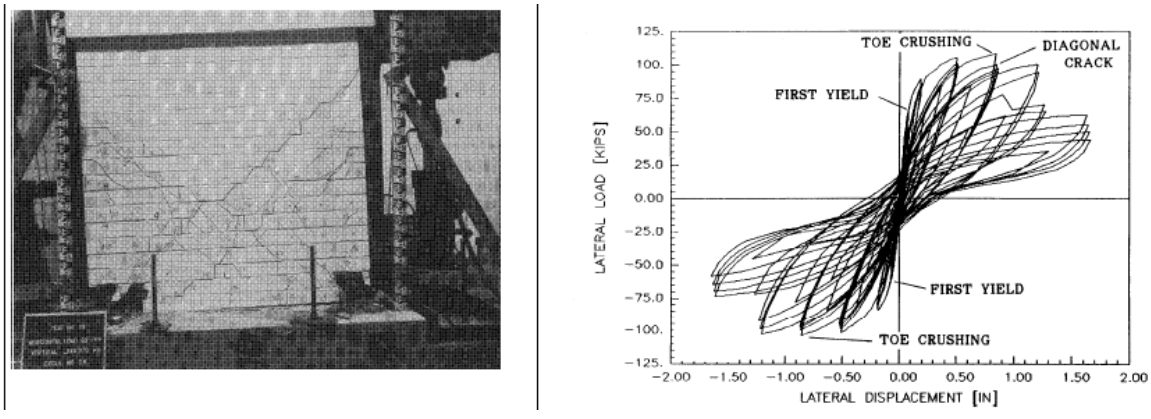

b)

Figure C-23. Cracking pattern and load-displacement curves for damaged masonry wall specimens: a) shear-dominant response, and b) flexure-dominant response (Shing et al., FEMA 307, reproduced by permission of the Federal Emergency Management Agency).

For the *flexure-dominant mechanism*, a drop in the stiffness immediately after the onset of cracking is not very significant. As can be seen from Figure C-23b, the stiffness drops after the yielding of vertical reinforcement takes place, and continues to drop with increasing inelastic lateral deformations (this depends on the ductility capacity of the wall under consideration). The specimen for which the results are shown in Figure C-23b showed yielding of vertical reinforcement and compressive crushing of masonry at the wall toes (Shing et al., 1989).

Note that the height of wall test specimens shown in Figure C-23 was 1.8 m (6 feet), thus a 2.5% drift ratio permitted by the NBCC 2005 for regular buildings corresponds to 1.8 inch displacement. It can be seen that the displacements and drift in these specimens are very low, particularly so for the shear-dominant specimen shown in Figure C-23a.

Evidence from studies that focus on quantifying the changes in in-plane wall stiffness under increasing lateral loading are limited, so CSA S304.1 and other masonry codes do not provide guidance related to this issue. Shing et al. (1990) tested a series of 22 cantilever block masonry wall specimens that were laterally loaded at the top, with a height/length aspect ratio of 1.0. Based on the experimental test data, they have recommended the following empirical equation for the lateral stiffness of a wall with a shear-dominant response

$$K_e = (0.2 + 0.1073 f_c) K_{shear} \le K_{el} \qquad (15)$$

where

$K_{shear} = \dfrac{E_m * t_e}{3 * \left(\dfrac{h}{l_w} \right)}$ is the shear stiffness of a wall/pier

h = wall height

l_w = wall length

t_e = effective wall thickness

f_c = axial compressive stress (MPa)

The above equation is based on the force/displacement measurements taken just after the first diagonal crack developed, in specimens with a height/length ratio of 1.0. For seismic applications where the walls are expected to yield in flexure before failing in shear, and the lateral stiffness is used to estimate the fundamental period of the structure and to determine the seismic displacements, it is more appropriate to determine the effective stiffness from a cracked section analysis at first yield of the tension reinforcement.

A study by Priestley and Hart (1989), based on the cracked transformed section stiffness at first yield of the tension reinforcement, recommends that the effective moment of inertia, I_e, of a wall can be approximated by:

$$I_e = \left(\frac{100}{f_y} + \frac{P_f}{f'_m A_e} \right) I_g \qquad (16)$$

where

f_y = steel yield strength (MPa)

P_f = factored axial load

A_e = effective cross-sectional area for the wall

f'_m = masonry compressive strength, and

$I_g = \frac{t_e * l_w^3}{12}$ is the gross moment of inertia of the wall.

Note that the first term in the bracket, $100/f_y$, is equal to 0.25 for $f_y = 400$ MPa (Grade 400 steel). The second term is a ratio of axial compressive stress in the wall, equal to P_f/A_e, and the masonry compressive strength, f'_m.

The above relation is based solely on consideration of flexural stiffness, and is a best fit relationship for several different values of height/length ratio (h/l_w), steel strength, vertical reinforcement ratio and axial load. Other considerations are whether the vertical reinforcement is uniformly distributed across the wall length or concentrated at the ends, and the effect of tension stiffening. The vertical reinforcement ratio is not included in the above expression, and as a result, the wall stiffness is overestimated for lightly reinforced walls and underestimated for heavily reinforced walls.

If it is assumed that wall cracking causes the same proportional decrease in the effective shear area as it does for the moment of inertia, then the stiffnesses can be combined to give the following equation for the reduced wall stiffness, K_{ce},

$$K_{ce} = (\frac{100}{f_y} + \frac{P_f}{f'_m A_e})K_c \qquad (17)$$

where

$$K_c = \frac{E_m * t_e}{\left(\frac{h}{l_w}\right)\left[4\left(\frac{h}{l_w}\right)^2 + 3\right]}$$

is the combined stiffness of an uncracked cantilever wall or pier, considering both the flexural and shear deformation components (refer to Section C.3.2 for the wall stiffness equations).

The terms in the large right hand bracket of the K_c equation give the comparative value of flexural deformation to shear deformation. At a h/l_w ratio of 1.0, flexure contributes 4/7 of the total deformation and shear 3/7, while at a h/l_w ratio of 0.5, shear contributes ¾ of the total defection.

The Priestley and Hart equation was obtained using experimental data related to cantilever wall specimens, however it may also be used for fixed-end walls. The stiffness equation for these walls, K_{fe}, is the same as for the cantilever walls, that is,

$$K_{fe} = (\frac{100}{f_y} + \frac{P_f}{f'_m A_e})K_f \qquad (18)$$

where

$K_f = \frac{E_m * t_e}{\left(\frac{h}{l_w}\right)\left[\left(\frac{h}{l_w}\right)^2 + 3\right]}$ is the stiffness of an uncracked fixed-end wall or a pier

A comparison of the proposed equations for a masonry block wall under axial compressive stress is presented in Figure C-24. The following values were used in the calculations: $f_y = 400$ MPa, P_f/A_e = 1 MPa, and f'_m = 10 MPa.

Note that the Shing equation is only shown for h/l_w up to 1.5 as it is based entirely on shear deformation. Since the Shing equation represents stiffness at first diagonal cracking, it is expected to give higher stiffness values than the Priestley-Hart equation. Use of the Priestley-Hart stiffness equation is recommended since it is valid for all h/l_w ratios.

The elastic uncracked stiffness could be used to distribute lateral seismic load to individual walls and piers, but the reduced cracked stiffness should be used for period estimation and deflection calculations.

The wall design deflections can be found from the following equation:

$$\Delta_{design} = \Delta_{el} * \frac{R_d * R_o}{I_E}$$

where

Δ_{el} = elastic deflections calculated using the reduced wall stiffness (K_{ce} or K_{fe}) and the factored design forces, and

$\frac{R_d * R_o}{I_E}$ = deflection multiplier to account for the effects of ductility, overstrength, and the building importance factor (see Section 1.5.11)

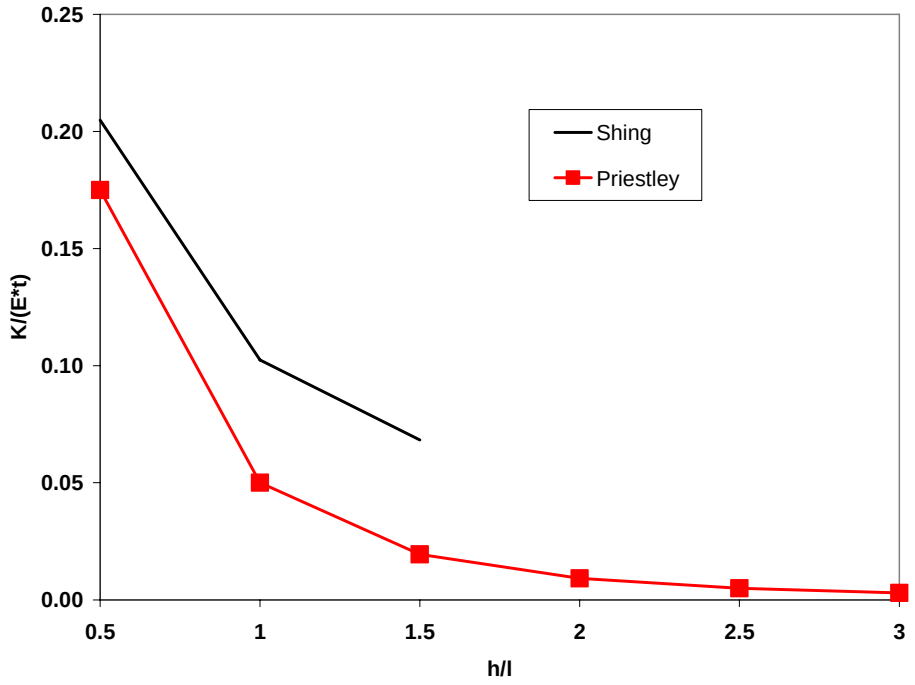

Figure C-24. A comparison of the stiffness values obtained using the Shing and Priestley-Hart equations.

TABLE OF CONTENTS – APPENDIX D

D Design Aids

Table D-1. Properties of Concrete Masonry Walls (per metre or foot length)[1]

Grouted Cells / metre		0.00	0.83	1.00	1.25	1.67	2.50	5.00
Cell/dowel Spacing (mm)		*none*	1200	1000	800	600	400	200
Nominal Size		***150***	**mm**		***6***	**inch**		
A_e	($mm^2 \times 10^3$)	52.0	66.7	69.6	74.0	81.3	96.0	140.0
	(in^2)	*24.6*	*31.5*	*32.9*	*35.0*	*38.4*	*45.4*	*66.2*
I_x	($mm^4 \times 10^6$)	172	181	183	186	191	201	229
	(in^4)	*126*	*133*	*134*	*136*	*140*	*147*	*168*
S_x	($mm^3 \times 10^6$)	2.46	2.59	2.62	2.66	2.73	2.87	3.27
	(in^3)	*45.8*	*48.2*	*48.7*	*49.5*	*50.7*	*53.3*	*60.8*
Weight	(kN/m^2)	1.90	2.09	2.13	2.19	2.29	2.49	3.08
	(psf)	*39.6*	*43.7*	*44.6*	*45.8*	*47.9*	*52.0*	*64.3*
Nominal Size		***200***	**mm**		***8***	**inch**		
A_e	($mm^2 \times 10^3$)	75.4	94.5	98.3	104.0	113.6	132.7	190.0
	(in^2)	*35.6*	*44.6*	*46.5*	*49.2*	*53.7*	*62.7*	*89.8*
I_x	($mm^4 \times 10^6$)	442	464	468	475	485	507	572
	(in^4)	*324*	*340*	*343*	*347*	*355*	*371*	*419*
S_x	($mm^3 \times 10^6$)	4.66	4.88	4.93	5.00	5.11	5.34	6.02
	(in^3)	*86.7*	*90.9*	*91.7*	*93.0*	*95.0*	*99.3*	*112.0*
Weight	(kN/m^2)	2.46	2.75	2.81	2.89	3.03	3.32	4.18
	(psf)	*51.4*	*57.4*	*58.6*	*60.4*	*63.4*	*69.4*	*87.3*
Nominal Size		***250***	**mm**		***10***	**inch**		
A_e	($mm^2 \times 10^3$)	81.7	108.1	113.4	121.3	134.5	160.9	240.0
	(in^2)	*38.6*	*51.1*	*53.6*	*57.3*	*63.5*	*76.0*	*113.4*
I_x	($mm^4 \times 10^6$)	816	872	883	900	928	984	1152
	(in^4)	*598*	*638*	*647*	*659*	*679*	*721*	*844*
S_x	($mm^3 \times 10^6$)	6.80	7.27	7.36	7.50	7.73	8.20	9.60
	(in^3)	*126.5*	*135.2*	*136.9*	*139.5*	*143.8*	*152.5*	*178.6*
Weight	(kN/m^2)	2.97	3.35	3.43	3.55	3.74	4.12	5.28
	(psf)	*62.0*	*70.0*	*71.7*	*74.1*	*78.1*	*86.1*	*110.3*
Nominal Size		***300***	**mm**		***12***	**inch**		
A_e	($mm^2 \times 10^3$)	88.3	121.9	128.6	138.7	155.5	189.2	290.0
	(in^2)	*41.7*	*57.6*	*60.8*	*65.5*	*73.5*	*89.4*	*137.0*
I_x	($mm^4 \times 10^6$)	1341	1456	1479	1514	1571	1687	2032
	(in^4)	*982*	*1066*	*1083*	*1108*	*1150*	*1235*	*1488*
S_x	($mm^3 \times 10^6$)	9.25	10.04	10.20	10.44	10.83	11.63	14.01
	(in^3)	*172.1*	*186.8*	*189.7*	*194.1*	*201.5*	*216.3*	*260.6*
Weight	(kN/m^2)	3.53	4.00	4.10	4.24	4.48	4.95	6.38
	(psf)	*73.7*	*83.6*	*85.6*	*88.6*	*93.6*	*103.5*	*133.3*
Note:	Assume Bond Beams at 2.4 m (8 ft) O.C.							
	Table based on Metric blocks and modules (190 mm high units)							
	Assumed Weight	22	kN/m3	140.4	pcf			

[1] Source: Masonry Technical Manual (MIBC, 2008, reproduced by permission of the Masonry Institute of BC)

Table D-2. c/l_w *ratio,* f_y *= 400 MPa*

ω	α										
	0.000	0.025	0.050	0.075	0.100	0.150	0.200	0.250	0.300	0.350	0.400
0	0.000	0.037	0.074	0.110	0.147	0.221	0.294	0.368	0.441	0.515	0.588
0.01	0.014	0.050	0.086	0.121	0.157	0.229	0.300	0.371	0.443	0.514	0.586
0.02	0.028	0.063	0.097	0.132	0.167	0.236	0.306	0.375	0.444	0.514	0.583
0.03	0.041	0.074	0.108	0.142	0.176	0.243	0.311	0.378	0.446	0.514	0.581
0.04	0.053	0.086	0.118	0.151	0.184	0.250	0.316	0.382	0.447	0.513	0.579
0.05	0.064	0.096	0.128	0.160	0.192	0.256	0.321	0.385	0.449	0.513	0.577
0.06	0.075	0.106	0.138	0.169	0.200	0.263	0.325	0.388	0.450	0.513	0.575
0.07	0.085	0.116	0.146	0.177	0.207	0.268	0.329	0.390	0.451	0.512	0.573
0.08	0.095	0.125	0.155	0.185	0.214	0.274	0.333	0.393	0.452	0.512	0.571
0.09	0.105	0.134	0.163	0.192	0.221	0.279	0.337	0.395	0.453	0.512	0.570
0.1	0.114	0.142	0.170	0.199	0.227	0.284	0.341	0.398	0.455	0.511	0.568
0.11	0.122	0.150	0.178	0.206	0.233	0.289	0.344	0.400	0.456	0.511	0.567
0.12	0.130	0.158	0.185	0.212	0.239	0.293	0.348	0.402	0.457	0.511	0.565
0.13	0.138	0.165	0.191	0.218	0.245	0.298	0.351	0.404	0.457	0.511	0.564
0.14	0.146	0.172	0.198	0.224	0.250	0.302	0.354	0.406	0.458	0.510	0.563
0.15	0.153	0.179	0.204	0.230	0.255	0.306	0.357	0.408	0.459	0.510	0.561
0.16	0.160	0.185	0.210	0.235	0.260	0.310	0.360	0.410	0.460	0.510	0.560
0.17	0.167	0.191	0.216	0.240	0.265	0.314	0.363	0.412	0.461	0.510	0.559
0.18	0.173	0.197	0.221	0.245	0.269	0.317	0.365	0.413	0.462	0.510	0.558
0.19	0.179	0.203	0.226	0.250	0.274	0.321	0.368	0.415	0.462	0.509	0.557
0.2	0.185	0.208	0.231	0.255	0.278	0.324	0.370	0.417	0.463	0.509	0.556

Input parameters:

$$\rho_{vflex} = \frac{A_{vt}}{t * l_w}$$

$$\omega = \frac{566.7 * \rho_{vflex}}{f'_m}$$

$$\alpha = \frac{1667 * P_f}{f'_m l_w t}$$

Units:

P_f (kN)

l_w, t (mm)

A_{vt} (mm^2)

f'_m (MPa)

Table D-3. Wall Stiffness Values $K/(E_m * t)$

h/l	Cantilever	Fixed
0.05	6.645	6.661
0.1	3.289	3.322
0.15	2.157	2.206
0.2	1.582	1.645
0.25	1.231	1.306
0.3	0.992	1.079
0.35	0.819	0.915
0.4	0.687	0.791
0.45	0.583	0.694
0.5	0.500	0.615
0.55	0.432	0.551
0.6	0.375	0.496
0.65	0.328	0.450
0.7	0.288	0.409
0.75	0.254	0.374
0.8	0.225	0.343
0.85	0.200	0.316
0.9	0.178	0.292
0.95	0.159	0.270
1	0.143	0.250
1.05	0.129	0.232
1.1	0.116	0.216
1.15	0.105	0.201
1.2	0.095	0.188
1.25	0.086	0.175
1.3	0.079	0.164
1.35	0.072	0.154
1.4	0.066	0.144
1.45	0.060	0.135
1.5	0.056	0.127
1.55	0.051	0.119
1.6	0.047	0.112
1.65	0.044	0.106
1.7	0.040	0.100
1.75	0.037	0.094
1.8	0.035	0.089
1.85	0.032	0.084
1.9	0.030	0.080
1.95	0.028	0.075
2	0.026	0.071

Cantilever model:

$$\frac{K}{E_m * t} = \frac{1}{\left(\frac{h}{l_w}\right)\left[4\left(\frac{h}{l_w}\right)^2 + 3\right]}$$

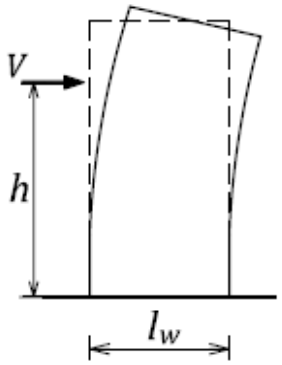

Fixed both ends:

$$\frac{K}{E_m * t} = \frac{1}{\left(\frac{h}{l_w}\right)\left[\left(\frac{h}{l_w}\right)^2 + 3\right]}$$

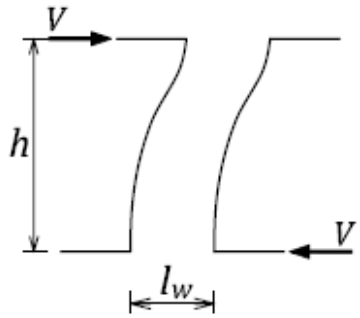

$E_m = 850 f'_m$ Modulus of elasticity

$G = 0.4E_m$ Modulus of rigidity (shear modulus)

$A_v = 5A/6$ Shear area

E Notation

$a_{\max}$ = maximum acceleration

a = depth of the compression zone (equivalent rectangular stress block)

a_w = clear distance between the adjacent cross walls

A_b = area of reinforcement bar

A_c = area of concentrated reinforcement at each end of the wall

A_d = area of distributed reinforcement along the wall length

A_e = effective cross-sectional area of masonry

A_g = gross cross-sectional area of masonry

A_L = area of the compression zone (flanged wall section)

A_r = response amplification factor to account for the type of attachment of equipment or veneer ties

A_{uc} = uncracked area of the cross-section

A_v = area of horizontal wall reinforcement

A_{vt} = total area of the distributed vertical reinforcement

A_v = shear area of the wall section

A_x = amplification factor at level x to account for variation of response with the height of the building (veneer tie design)

b = effective width of the compression zone

b_{actual} = actual flange width

b_c = critical wall thickness

b_T = overhanging flange width

b_w = overall web width (shear design)

B = torsional sensitivity factor

c = neutral axis depth (distance from the extreme compression fibre to the neutral axis)

C = compressive force in the masonry acting normal to the sliding plane

C_m = the resultant compression force in masonry

C_h = compressive force in the masonry acting normal to the head joint

C_p = seismic coefficient for a nonstructural component (veneer tie design)

d = effective depth (distance from the extreme compression fibre to centroid of tension reinforcement)

d_v = effective wall depth for shear calculations

d' = distance from the extreme compression fibre to the centroid of the concentrated compression reinforcement

D_{nx} = plan dimension of the building at level x perpendicular to the direction of seismic loading being considered

e = load eccentricity

e_a = accidental torsional eccentricity

e_x = torsional eccentricity (distance measured perpendicular to the direction of earthquake loading between the centre of mass and the centre of rigidity at the level being considered)

E_f = modulus of elasticity of the frame material (infill walls)

E_m = modulus of elasticity of masonry

f_t = flexural tensile strength of masonry (see Table 5 of CSA S304.1-04)

f'_m = compressive strength of masonry normal to bed joints at 28 days (see Table 4 of CSA S304.1-04)

f_y = yield strength of reinforcement

F = force

F_t = a portion of the base shear V applied at the top of the building

F_{el} = elastic force

F_a = acceleration-based site coefficient

F_v = velocity-based site coefficient

F_x = seismic force applied to level x

F_y = yield force

G = modulus of rigidity for masonry (shear modulus)

h = unsupported wall height/height of the infill wall

h_w = total wall height

h_n = building height

h_s = storey height

h_x = height from the base of the structure up to the level x

I_b = moment of inertia of the beam

I_c = moment of inertia of the column

I_E = earthquake importance factor of the structure

J = numerical reduction coefficient for base overturning moment

k = effective length factor for compression member

K = stiffness

l = length of the infill wall

l_d = design length of the diagonal strut (infill wall)

l_p = plastic hinge length

l_s = length of the diagonal strut

l_w = wall length

L_n = clear vertical distance between lines of effective horizontal support or clear horizontal distance between lines of effective vertical support

M = mass

M_f = factored bending moment

M_r = factored moment resistance

M_n = nominal moment resistance

M_p = probable moment resistance

M_v = factor to account for higher mode effect on base shear

N = axial load arising from bending in coupling beams or piers

p_f = distributed axial stress

P_d = axial compressive load on the section under consideration

P_{cr} = critical axial compressive load

P_{DL} = dead load

P_{fb} = the resultant compression force (flanged walls)

P_r = factored axial load resistance

P_1 = compressive force in the unreinforced masonry acting normal to the sliding plane

P_2 = compressive force in the reinforced masonry acting normal to the sliding plane

P_h = horizontal component of the diagonal strut compression resistance (infill walls)

P_v = the vertical component of the diagonal strut compression resistance (infill walls)

P_{ult} = ultimate tie strength

R_d = ductility-related force modification factor

R_o = overstrength-related force modification factor

R_p = element or component response modification factor (veneer tie design)

s = reinforcement spacing

$S(T)$ = design spectral acceleration

$S_a(T)$ = 5% damped spectral response acceleration

S_e = section modulus of effective wall cross-sectional area

S_p = horizontal force factor for part or portion of a building and its anchorage (veneer tie design)

t = overall wall thickness

t_e = effective wall thickness

t_f = face shell thickness

T = fundamental period of vibration of the building

T_x = torsional moment at level x

T_r = the resultant force in steel reinforcement

T_y = factored tensile force at yield of the vertical reinforcement

v_f = distributed shear stress

v_m = masonry shear strength

$v_{\max}$ = maximum velocity

V = lateral earthquake design force at the base of the structure

V_e = lateral earthquake elastic force at the base of the structure

V_f = factored shear force

V_{nb} = the resultant shear force corresponding to the development of nominal moment resistance M_n at the base of the wall

V_m = masonry shear resistance

V_r = factored shear resistance

$\overline{V_s}$ = average shear wave velocity in the top 30 m of soil or rock

V_s = factored shear resistance of steel reinforcement

w = diagonal strut width (infill walls)

w_e = effective diagonal strut width (infill walls)

W = seismic weight, equal to the dead weight plus some portion of live load that would move laterally with the structure

W_p = weight of a part or a portion of a structure (veneer tie design)

W_x = a portion of seismic weight W that is assigned to level x

α_h = vertical contact length between the frame and the diagonal strut (infill walls)

α_L = horizontal contact length between the frame and the diagonal strut (infill walls)

β = damping ratio

β_d = ratio of the factored dead load moment to the total factored moment

β_1 = ratio of depth of rectangular compression block to depth of the neutral axis

γ_g = factor to account for partially grouted or ungrouted walls that are constructed of hollow or semi-solid units

$\delta_{\max}$ = the maximum storey displacement at level x at one of the extreme corners in the direction of earthquake

δ_{ave} = the average storey displacement determined by averaging the maximum and minimum displacements of the storey at level x

Δ = lateral displacement

Δ_p = plastic displacement

Δ_y = displacement at the onset of yielding

Δ_{el} = elastic displacement

$\Delta_{\max}$ = maximum displacement

Δ_u = inelastic (plastic) displacement

ε_m = the maximum compressive strain in masonry

ε_s = strain in steel reinforcement

ε_y = yield strain in steel reinforcement

χ = factor used to account for direction of compressive stress in a masonry member relative to the direction used for determination of f'_m

φ = curvature

φ_u = ultimate curvature

φ_y = yield curvature corresponds to the onset of yielding

ϕ_{er} = resistance factor for member stiffness

ϕ_m = resistance factor for masonry

ϕ_s = resistance factor for steel reinforcement

ϕ = resistance factor

ρ_v = vertical reinforcement ratio

ρ_h = horizontal reinforcement ratio

μ = coefficient of friction

μ_Δ = displacement ductility ratio (Chapter 1)

μ_φ = curvature ductility ratio

μ_Δ = displacement ductility ratio

θ = angle of diagonal strut measured from the horizontal

θ_e = elastic rotation

θ_p = plastic rotation

ω = natural frequency